

Simulating Neutrino Oscillations in a Quantum Computer
&
Studying Entanglement Dynamics

Navaneeth Krishnan M
CUSAT, India.

June 3, 2021

Contents

1	Quantum Simulations: An Overview	12
1.1	Digital Quantum Simulations	14
1.2	Analog Quantum Simulations (AQS)	16
1.3	Quantum-Information-Inspired Algorithms for Classical Simulation of Quantum Systems	18
2	Neutrino Oscillation	20
2.1	Neutrino Flavour Oscillation in Vacuum	21
2.1.1	Theory of Flavour Oscillation	22
3	Entanglement in Neutrino Oscillations	29
3.1	Single Particle Entanglement	30
3.2	Entanglement in Neutrinos	31
3.3	Entanglement Measurement	32
3.3.1	Pure and Mixed States	32
3.4	Entanglement Entropy	34
3.5	Measurement of Entanglement in Neutrinos	35
4	Neutrino Oscillation in a quantum processor	38
4.1	Simulation of Two Flavour Oscillation	40

4.2	Simulation of Three Flavour Neutrino Oscillation	41
4.3	Measuring Entanglement Using Simulation	44
5	Simulation Results	47
5.1	Two Flavour Oscillations: Simulation Results	47
5.1.1	Simulation Using QASM Simulator	47
5.1.2	Simulation Using IBM Quantum Computer	49
5.1.3	Entanglement Studies	50
5.2	Three Flavour Oscillation: Simulation Results	52
5.2.1	Simulation Using QASM Simulator	53
5.2.2	Simulation Using IBM Quantum Computer	53
5.2.3	Entanglement Studies	54

List of Figures

1.1	Scheme for analog simulations	16
4.1	Circuit simulating two flavour oscillation[1]	42
4.2	Gate arrangement for realizing PMNS matrix[1]	43
4.3	Circuit for simulating three flavour oscillation[1]	44
5.1	Disappearance probability in $e - \mu$ system as a function of energy (in QASM simulator)	48
5.2	Disappearance probability in $e - \mu$ system as a function of energy (in Quantum computer)	49
5.3	Linear entropy of $e - \mu$ system as a function of energy (in QASM simulator)	50
5.4	Linear entropy of $e - \mu$ system as a function of energy (in quantum computer)	50
5.5	Entanglement in the $e - \mu$ system (in QASM simulator)	51
5.6	Entanglement in the $e - \mu$ system (in Quantum computer)	51
5.7	Three flavour oscillation probability as function of time (in QASM simulator)	53
5.8	Three flavour oscillation probability as function of time (in Quantum computer)	54
5.9	Linear entropy of 3-flavour system as a function of energy (in QASM simulator)	55

5.10	Linear entropy of 3-flavour system as a function of energy (in quantum computer)	55
5.11	Global entanglement in the 3-flavour system (in QASM simulator).	56
5.12	Global entanglement in the 3-flavour system (in Quantum computer).	56

Introduction

“ Can physics be simulated by a universal computer? [...] the physical world is quantum mechanical, and therefore the proper problem is the simulation of quantum physics [...] the full description of quantum mechanics for a large a system with R particles [...] has too many variables, it cannot be simulated with a normal computer with a number of elements proportional to R [...] but it can be simulated with] quantum computer elements. [...] Can a quantum system be probabilistically simulated by a classical (probabilistic, I’d assume) universal computer? [...] If you take the computer to be the classical kind I’ve described so far [...] the answer is certainly, No! “

-Richard P Feynman [2][3]

The primary aim of any sort of simulation is to solve the differential equation that governs the dynamics of the system. One of the most simple example of such an equation is the Newtons equation of motion,

$$m \frac{d^2x}{dx} = F \quad (1)$$

Generally, the initial state of the system would be input to the problem. Using simulations, one aims to predict the state of the system at a later time or position. The first step in doing any simulation is the encoding of state of system digitally, which more often involves some approximation. Using the encoding scheme, we have to prepare the initial state of system. Then one has to discretize the dynamical differential equation in space and time. Discretization should be done in such a way that the iterative application of a procedure should evolve the state from initial to final conditions. The accuracy of output state predicted by the simulator depends upon discretization length. Theoretically, as the length of discretization decreases the result would be more accurate. But while computing we need to consider other errors that can arise while decreasing the discretization length is taken. Thus often an optimum value of discretization length. Now, Why this approach works?. This works because the error is bounded and not considerably grows as the number of

iterations increases. Further, only those system that can be efficiently described can be simulated efficiently. Thus there are systems where such an approach fails.

Now comes the question of whether we can simulate a quantum system using a classical simulator. The short answer is yes. But it should be noted that often such simulations are inefficient and fail when the number of particles in the system is very high. When we analyse the problem of simulating a quantum system, for most of simple quantum systems, the evolution is governed by the time-independent Schrodinger equation.

$$i\hbar \frac{d}{dt} |\psi\rangle = \hat{H} |\psi\rangle \quad (2)$$

On the position basis, the above equation will be

$$i\hbar \frac{\partial}{\partial t} \psi(x) = \left[-\frac{\partial^2}{\partial x^2} + V(x) \right] \psi(x) \quad (3)$$

Where $\langle x|\psi\rangle = \psi(x)$.

Assume that we wish to simulate a simple two-level system (Qubit) that obeys time-independent Schrodinger equation. For such a system, we have to solve two differential equations to simulate it. If it is a two-qubit system then there would be four equations and so on. Thus, a general system of n qubits 2^n differential equations must be solved to simulate it. This exponential explosion in the equation is unavoidable unless we employ some approximate methods like Monte Carlo methods [4] which considerably reduce the number of equations. Such classical stochastic methods would allow us to evaluate the phase-space integrals of many-body quantum systems in polynomial time. But these methods are efficient while the function being integrated does not change its sign. Thus while using such methods, sampling of the function is done in a relatively small number of points. For systems like fermionic or frustrated systems, the integrals encounter the problem of sampling with non-positive semi-definite functions (referred to as negative sign problem [5][6]) which cause an exponential increase in computation time as the number of particles increases. Thus in such systems, Monte Carlo methods are shown to be inefficient. Other than Monte Carlo methods, there are methods like Density Functional Theory (DFT) [7], mean-field theories, Green function-based methods, many-body perturbation theories [8] etc. These methods also have their own limitations.

Richard P Feynman was one of the persons who put forward a solution to this problem. He said that “*Let the computer itself be built of quantum mechanical elements which obeys quantum mechanical laws*” [2]. Feynman realized that such a quantum system - which later called a quantum computer - would be able to handle the exponential explosion of parameters that happen while solving a large number of equations without using an exponentially large number of physical resources. Even

though Feynman proposed such a radical idea, he was not aware of how to realise simulations in such controllable quantum systems. More than a decade later, it was Lloyd who showed that quantum computer could act as a universal quantum simulator [9]. Here the term “universal” is used in the sense that the same system can be used to simulate vastly different problems. Of course, one has to make adjustments in the algorithm according to problem.

Even though the quantum computer was proposed to simulate quantum mechanics, its uses extend far beyond it. The past three decades have revealed the true power of a quantum computer. Nowadays quantum computing and quantum information itself a topic of research. Further, it became later clear that we don’t always need a quantum computer for implementing quantum simulations. For simulating a particular quantum system, we only need a simple quantum system that has similar time evolution. That is, simple quantum devices that mimic the time evolution of other quantum systems can be used as simulators. But the drawback of such an approach is that such a simulator would be problem-specific (not universal). On the bright side, such simple systems can be easily controlled and designed compared to sophisticated quantum computers.

Based on the approach, we can broadly classify the quantum simulations into kinds; Analog Quantum Simulation (AQS) and Digital Quantum Simulations (DQS). In DQS we use quantum computers as simulators. Here we encode the time evolution of the quantum system in a quantum circuit comprising qubits and quantum gates. The circuit is designed in such a way that the output of the circuit gives the time evolved state of the system under study. A similar but different approach is taken in Analog Quantum Simulations. In AQS, a simple quantum system that is controllable is created depending upon the problem. This system is designed in such a way that it would mimic the time evolution of the system under study. Thus in this approach, simulations are done using a simple quantum system as simulators.

In recent years, the field of quantum simulations has gained momentum. The sudden spike in interest is two folds. The first one is its wide range of application. For instance, quantum simulations can be used in condensed matter for studying many difficult problems like quantum phase transitions, high T_c superconductivity, quantum magnetism etc. Other potential applications include fields like high energy physics, nuclear physics, cosmology, quantum chemistry etc. The second factor that accelerated the growth of quantum simulations is the recent progress in the field of quantum technologies. Recent years have witnessed development in different types of realization of quantum computers. Nowadays quantum computers are publicly accessible. Quantum simulators which can be used to perform simulations repeatedly are now available. Technologies to maintain coherent control over the system and

to perform measurements have matured enough to make it possible.

In near future, quantum simulations will become a prominent tool for research for a wide variety of fields. In this milieu, the study of quantum simulations holds importance. This was the motivation for us to conduct this study. Here we are interested in the digital quantum simulations of phenomena called Neutrino oscillation. We use the quantum computing services provided by IBM to carry out our simulations. The scheme for such a simulation was put forward by Argüelles and Jones in 2017 [1]. They have encoded neutrino oscillation into a quantum circuit. Time evolution of the qubits is done by applying unitary single and two-qubit gates. The exact scheme will be discussed in the following sections 4 5.

In nature, neutrinos are produced in three distinct flavours electron, muon and tau. Neutrinos are produced through weak interactions. As neutrino beam propagates from source to detector neutrino flavour oscillate between the three flavours. The first evidence of neutrino exhibit flavour oscillation from the famous Ray Davis Homestake experiment [10]. He reported a deficit in the flux of solar neutrinos (electron neutrinos) from the value predicted by the Standard model. He used a chlorine-based detector and obtained a flux that was three times less than that of the theoretical value. This observation of Ray Davis later came to be known “Solar Neutrino Problem”. For the contributions in the field of astrophysics, Ray Davis was awarded the Nobel prize in Physics in 2002.

Following the Homestake experiment, different sort of powerful detectors was set up and studied the problem. All the experiments confirmed the deficit of neutrinos in the solar flux. Ray Davis performed his experiment in the 1960s. Interestingly, the idea of neutrino oscillation was put forward by Pontecorvo in 1957 [11]. Thus one can say that solution existed even before the problem. But in Pontecorvo’s version neutrino-anti neutrino undergo oscillation. He put forward this theory in analogy with the neutral kaon mixing that was known way before. Although such oscillations do not occur in nature, this formed a key conceptual foundation in developing the theory for neutrino oscillation. The theory for neutrino flavour oscillation was put forward first by Maki, Nakagawa, Sakata in 1962 [12] which was later elaborated by Pontecorvo in 1967 [13]. The solar neutrino deficit observed only a year after that. The solar neutrino problem baffled scientists for a long time. It was the team of Canadian scientists lead by Arthur B McDonald in Sudurbary Neutrino Observatory (SNO) that put an end to the mystery. They experimentally verified that electron neutrino produced in the sun undergo flavour oscillations. The deficit in the number of electron neutrinos was because neutrinos undergo flavour change while travelling to Earth [14]. At the same time, a group of Japanese scientist lead by Takaaki Kajita verified neutrino oscillation by studying atmospheric neutrinos.

Atmospheric neutrinos were produced when cosmic rays hit the Earth's atmosphere. When it travels to the Earth's surface they undergo flavour oscillations. The team led by Kajita was able to detect these flavour oscillations. For the experimental verification of neutrino flavour oscillation, both Kajita and McDonald was awarded the Nobel prize in physics in 2015.

The verification that neutrinos can undergo oscillations comes with great consequences. It was known that neutrinos can undergo flavour oscillation only if they have mass. But according to the Standard Model, neutrinos are massless. Thus the phenomenon of neutrino oscillation insists on the modification of the standard model. Even though there are some minimal extensions of the Standard model to accommodate neutrino masses, exact theory is unknown. Neutrino oscillation experiments gives us mass squared splittings and mixing angles (will discuss it later). But till now the actual mass of the three neutrinos are still unknown. Thus the study of neutrino oscillation is a door to explore physics outside the standard model.

In this work, we performed simulation of the time evolution of a neutrino flavour state. During such simulations we were able to observe neutrino flavour oscillations. But the application of DQS extends more than the temporal evolution of the state of the system. DQS can be used to obtain certain properties of a quantum system. It has been shown that using DQS we can estimate the eigenvalues of the operators including Hamiltonian of the system. For example, Abrams and Lloyd have put forward an algorithm to find eigenvalues and eigenvectors of Hamiltonian [15]. They have proposed an algorithm that uses quantum fast Fourier transform to evaluate eigenvalues and eigenstates. Similarly, Aspuru-Guzik *et al.* by applying a recursive phase estimation algorithm have calculated the molecular ground state energies of lithium hydride and water molecule [16]. It has been also shown that DQS can be used to compute the partition function of the system [17]. Moreover, people have shown that classical physics can efficiently be simulated by quantum computers [18][19].

Here we used the DQS of neutrino oscillation to study the entanglement between different neutrino flavours. Blasone *et al.* through a series of papers [20][21][22][23], have proposed the existence of single particle entanglement in neutrinos. It was van Enk who proposed single particles can have entanglement [24][25][26]. He explained single particle entanglement in the context of single photons. Blasone *et al.* extended these concepts into the case of neutrinos. They also provided scheme to quantify the degree of entanglement in the system. They used a measure called *entanglement entropy* to quantify the entanglement. We applied their results in to our circuit and were able to accurately predict the entanglement dynamics of the system.

This report is organized as follow. In the first chapter [1], we provide a brief introduction to quantum simulations. Different types of approach for performing quantum simulations are discussed in this chapter. The second chapter [2] is dedicated for the discussion of neutrino oscillation. In this section, we discuss the neutrino oscillation theory (both two flavour and three flavour case) relevant for performing quantum simulations. In the following chapter [3], we discuss about the entanglement in the neutrino. Chapter [4] and Chapter [5] deals with the simulation of neutrino in a quantum computer. The scheme of performing such a simulation is given in the fifth chapter. The following chapter contains the results of the simulations performed. The conclusions and outlook is given in the concluding section.

Chapter 1

Quantum Simulations: An Overview

Simulating a quantum system by quantum mechanical means is defined as quantum simulation. For performing simulations, we need a quantum simulator. By definition, a quantum simulator is a controllable quantum system that can simulate or mimic other quantum systems. As discussed earlier, based on the type simulator used we can classify simulations as Digital and Analog quantum simulations. There is one more type of simulation method that belongs to the class of quantum simulations. It is called “Quantum Information inspired algorithms for classical simulations of quantum systems”. We will briefly discuss all of them in the following sections. Before that, we provide a bit more explanation on the advantage of quantum simulation over classical simulation.

As we discussed in the introduction simulating a system often include three steps: preparation of the initial state, time evolution of the state and measurement of the final state. Let the system we want to simulate be a system of N spin half particles. The system is described by state vector $|\psi\rangle$ at some time t . We have to encode the state first into the simulator. If we perform classical simulation, to encode $|\psi\rangle$ we need to store 2^N numbers in memory. The 2^N numbers represents the complex probability amplitudes of different spin configuration. Here we implicitly assume that spins do not have motional degrees of freedom. Now to get a physical sense of the problem, let us fix the value $N = 40$. Then we have to store $2^{40} \approx 10^{12}$ numbers for encoding $|\psi\rangle$. If we assume single-precision (7 decimal digits of precision), we would approximately need $\sim 3 \times 10^{13}$ bits. In terms of memory, it would correspond to 4TB (terabytes) memory [9][6]. If we double the number of spins it would require $\sim 3 \times 10^{25}$ bits (or 5×10^{12} TB). Now, while using a quantum computer, we only need N qubits to represent N spins. Thus a system of 40 spins can be represented

by a 40-qubit (5 quantum byte) register. Further, the quantum computer provides exponential compression of the memory space required. Recently a research group have shown that it only takes $\log_2[N+1]$ qubits to store N identical qubits [27]. That is, it only takes 10-qubit memory to store 1000 identical qubits and 11-qubit memory for 2000 qubits and so on. It is evident that in classical simulations, an exponential number of resources are needed (usually referred as *exponential explosion*).

Now for doing simulations, if we consider the most general case, we have to apply an arbitrary unitary transformation to the initial state. This unitary transformation matrix would be realised by logical gates in classical computation and would be replaced by quantum gates in quantum computation. Interestingly, as noted by Lloyd [9], the number of quantum gates required to an arbitrary unitary transformation is of the same order as logical gates required in classical computation. Thus at first glance, one would sceptical about the quantum advantage. But it should be noted that there a small difference between what we said and what Feynman proposed. Feynman conjectured that systems that evolve according to local interactions can be efficiently simulated by a quantum computer. Such a system which Feynman referring was not that undergoing an arbitrary unitary transformation. We are interested in the time evolution of system. Such a transformation is not arbitrary. In general, any systems that are consistent with Special and General Relativity evolve according to the local interactions [9]. Hamiltonian of such system will be of the form,

$$H = \sum_{l=1}^M H_l \quad (1.1)$$

Where H_l represents corresponds to local interaction Hamiltonian. For such type of systems, Lloyd has shown quantum simulations are more efficient than classical simulations [9].

The next obvious step of a simulation is the measurement of the final state. While doing the simulation using a classical computer it is not a big task. Technology has developed so much and we can considerably reduce readout errors in classical computers. But when it comes to a quantum computer, measurement isn't a walk in the park. Measurement is the only non-unitary transformation that we apply to the qubit. Direct measurement of the state of the qubit destroys its quantum nature. Also during measurement, due to interaction with outside, decoherence can happen to the qubit. Decoherence would induce errors in our measurement result. To prevent this we usually perform non-demolition measurements are used. it would not alter the state of the qubit. In such sort of measurements simulators have less interaction with their surroundings. Thus quantum information would be preserved and qubits would remain coherent.

The decoherence and thermal effects affecting the simulator can be exploited to mimic decoherence effects of the system we study. The feature set apart quantum simulation from its classical counterpart. Thus in short in instances we have to simulate a quantum system, quantum simulations outperform classical simulations. Quantum simulation prevents the exponential explosion. This is inevitable in classical simulation as the number of quantum variables increases. With that said, we are now going to discuss different types of quantum simulations.

1.1 Digital Quantum Simulations

Circuit (quantum circuit) based simulation of a quantum system is called Digital Quantum Simulation. In this approach, we create a quantum circuit using qubits and quantum gates that mimic the time evolution of the system. For building such circuits, we first have to encode the state vector $|\psi\rangle$ in the computational basis. If we take the example of the system of N spins, it can be encoded using the scheme,

$$|\uparrow\rangle \rightarrow |1\rangle ; |\downarrow\rangle \rightarrow |0\rangle$$

Using the encoding scheme, we need to initialize the state of the system in the quantum register. This is called initial state preparation. It should be noted that encoding scheme may vary from one system to other. In many cases, initial state preparation is not a piece of cake. Efficient algorithms initializing the state often will not be available.

To get state of the system at time t , we have to apply the time evolution operation $\exp(-i\hbar Ht)$ to initial state $|\psi(0)\rangle$. The time evolution operator is unitary. In principle, any unitary operation can be represented by using quantum gates. Thus in DQS, time evolution operation is realised using quantum gates. During simulation, we apply a time-ordered sequence of gates to the initial state created.

Now, finding an efficient decomposition of Hamiltonian in quantum gate basis is itself a difficult problem. Most of the time evolution we implement would be an approximation of actual evolution. Also as Feynman pointed out, not all systems cannot be simulated. DQS can only be applied to a system whose Hamiltonian can be written as a sum of many local interactions. Form of such a hamiltonian is given by equation,

$$H = \sum_{l=1}^M H_l \quad (1.2)$$

Examples of such systems include the Hubbard model, Ising model etc.

If $[H_l, H_{l'}] = 0$ for all l and l' , then time evolution operator will be,

$$U = \prod_l e^{-i\hbar H_l t} \quad (1.3)$$

In such cases, the decomposition in terms of gates is straight forward can be easily done. Unfortunately for most of the cases of physical interest $[H_l, H_{l'}] \neq 0$. Then we have to resort to approximate methods for decomposition. In such cases, We discretize the evolution time into a large number of steps. Each step is of duration Δt . Then U can be written as,

$$U = [e^{-i\hbar H \Delta t}]^{\frac{t}{\Delta t}} \quad (1.4)$$

Using approximate methods like the first order Trotter formula we can decompose $\exp(-i\hbar H \Delta t)$ into quantum gates.

$$U(\Delta t) = e^{-i\hbar \sum_l H_l \Delta t} = \prod_l e^{-i\hbar H_l \Delta t} + \mathcal{O}((\Delta t)^2) \quad (1.5)$$

As a result when $\Delta t \rightarrow 0$.

$$U(\Delta t) \approx \prod_l e^{-i\hbar H_l \Delta t} \quad (1.6)$$

Now, to have high accuracy, Δt should be very small which in turn increases the number of gates. But in the quantum computers now available, the error increases with the number of gates applied. So in a practical scenario, we can only approximately decompose $\exp(-i\hbar H \Delta t)$. Further, there are results that emphasising the shortcomings of first-order Trotterization [28][29]. They have shown that decomposition can be more efficient by including higher order terms. Discussions about such methods can be found in [3].

After time evolution, we have to get back the output state from the circuit. In general, to completely reconstruct the state we use a technique called Quantum State Tomography (QST). In QST, we make many identical copies of the system. Then we perform a series of measurement along with different bases. To have a minimalistic understanding of how this method works, it useful to consider the parable “Blind men and an elephant”. In the parable, 5 blind men describe a different aspect of the elephant. Combining all of their observation would give the whole picture of an elephant. Similarly, a series of measurements on identical copies of the state each allow a glimpse into a distinct aspect of a quantum state’s reality. Each new measurement illuminates a different dimension of an unknown state. But while this method, the resources required would grow exponentially with the size of the system. So in most cases, projective measurements are done at the end of the circuit. In this sort of measurement, the state of the system is projected to a computational basis while measuring.

1.2 Analog Quantum Simulations (AQS)

Simulation of a quantum system using another quantum system that mimics the time evolution of the former is called Analog Quantum Simulations. A general scheme for AQS is given in the figure.

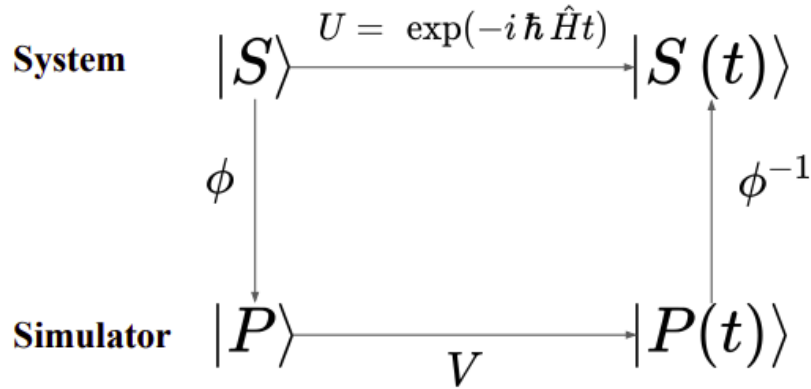


Figure 1.1: Scheme for analog simulations

$|S\rangle$ and $|S(t)\rangle$ represent the initial and final state (time evolved state) of system. Similarly, $|P\rangle$ and $|P(t)\rangle$ represent initial and final state of the simulator. Here the system is mapped to the simulator via an invertible map ϕ (operator). This mapping determines the correspondence between the states and operators of the system and simulator.

If we follow such a scheme described by figure 1.1, the evolution operator U and V would be connected by,

$$V = \phi U \phi^{-1} \quad (1.7)$$

If mapping is unitary, we can write,

$$V = e^{-i\hbar H_{sim} t} \quad (1.8)$$

Where $H_{sim} = \phi H_{sys} \phi^{-1}$.

Thus while simulation we map the initial state $|S\rangle$ to $|P\rangle$

$$|P\rangle = \phi |S\rangle \quad (1.9)$$

Then simulator is allowed to time evolve $|P\rangle \xrightarrow{V} |S\rangle$. After time evolution final state $|P(t)\rangle$ is mapped back to $|S(t)\rangle$.

$$|P(t)\rangle = \phi^{-1} |S(t)\rangle \quad (1.10)$$

Thus eventually we get back the time evolution of the system $|S\rangle \rightarrow |S(t)\rangle$.

Now we are going to discuss a very simple scheme of mapping between quantum system and simulator. The scheme we are discussing is proposed by Somaroo et al. (1999)[30] for simulating a quantum harmonic oscillator on two proton nuclear spins in 2,3-dibromothiophene. Note that here the number of states available for QHO is restricted to 4. The convenient unitary mapping of system and simulator is,

$$|n=0\rangle \leftrightarrow |\uparrow\uparrow\rangle |n=1\rangle \leftrightarrow |\uparrow\downarrow\rangle |n=2\rangle \leftrightarrow |\downarrow\uparrow\rangle |n=3\rangle \leftrightarrow |\downarrow\downarrow\rangle$$

One doesn't need to have followed this mapping. The mapping presented above is simple and straight forward.

The time evolution operator of QHO is given by

$$U = e^{-i\hbar H_{QHO}t} \equiv \exp \left[-i \left(\frac{1}{2} |0\rangle \langle 0| + \frac{3}{2} |1\rangle \langle 1| + \frac{5}{2} |2\rangle \langle 2| + \frac{7}{2} |3\rangle \langle 3| \right) \hbar\omega t \right] \quad (1.11)$$

Where ω is the oscillatory frequency. From this, we can find the time evolution of the simulator.

$$V = e^{-i\hbar H_{sim}t} \equiv \exp \left[-i \left(\frac{1}{2} |\uparrow\uparrow\rangle \langle \uparrow\uparrow| + \frac{3}{2} |\uparrow\downarrow\rangle \langle \uparrow\downarrow| + \frac{5}{2} |\downarrow\uparrow\rangle \langle \downarrow\uparrow| + \frac{7}{2} |\downarrow\downarrow\rangle \langle \downarrow\downarrow| \right) \hbar\omega t \right] \quad (1.12)$$

In Pauli basis $\sigma_x, \sigma_y, \sigma_z, I$, equation 1.12 can be rewritten as ,

$$V = \exp \left[i \left(\sigma_z^2 (1 + \frac{1}{2} \sigma_z^2) - 2 \right) \omega t \right] \quad (1.13)$$

Thus the simulator evolves according to equation 1.13. At the end of the simulation, final state of the simulator is measured. The resultant state is mapped back into the QHO state.

Sometimes we can simulate not able to simulate the entire system. But mapping can be done in such a way that it could be used to study some characteristic of the system. In general, the mapping we use depends upon the characteristic of the system we intend to study and the properties of the simulator. In AQS the physical quantities can be measured directly from the simulator. Since it is analogous to the system, measurement results yield information about the system. This is an added advantage since in DQS we need to computationally manipulate the measurement results. Also in AQS even if there are we can use it to perform qualitative studies. But the error rate should be below a tolerance level. In such cases, AQS can be used to investigate properties like phase transition.

Now in the example, we have shown, the mapping was simple and straight forward. But generally, this is not the case. Sometimes clever mapping schemes have to be formulated to efficiently simulate a system. Further discussion in this direction can be seen in the reference [6].

1.3 Quantum-Information-Inspired Algorithms for Classical Simulation of Quantum Systems

In this mode of approach, classical algorithms are used in the simulation of the quantum many body systems. But as discussed before, normal classical algorithms are prone to exponential explosion. Here in order to prevent this and to efficiently perform simulations we seek the assist of quantum information theory. First approach in this direction was done by Verstraete *et al.*(2004), they analysed the Density Matrix Re-normalization Method from a quantum information perspective [31].

This new hybrid class of algorithms help in efficient simulations of quantum lattice systems. Moreover, these methods can be combined with Monte Carlo Techniques to improve its efficiency. For example, it has been shown the quantum version of Metropolis algorithm overcomes the sign problem that we discussed before [32].

Chapter 2

Neutrino Oscillation

A neutrino (ν) is an elementary particle with a spin of $\frac{1}{2}$. It undergoes interaction only via the weak interaction and gravity. It was Pauli who proposed neutrino. According to him, neutrino was a non-interacting, neutral particle. He proposed existence of such a to recover conservation laws in the case of beta decay. At that time beta decay were appearing to energy, momentum, and angular momentum conservation laws. Even though they are abundant in-universe since they undergo only weak interaction, they rarely interact with matter and thus are incredibly difficult to detect. Therefore first detection of neutrino only occurred 25 years after it was first proposed. First detection of neutrinos was made by two American physicists Clyde Cowan and Frederick Reines. The detected anti neutrinos which were emitted by a nuclear reactor. For this discovery Frederick Reines was awarded the Nobel Prize in Physics in 1995.

During weak interactions neutrinos are created along with a corresponding charged lepton. The flavour of neutrino produced depends upon the lepton produced. They were proposed to be a massless particle. But it was later found that neutrinos do have mass. But till now we are not able to pinpoint the exact mass of a neutrino. This is because the flavour state of neutrino does not coincide with its mass states. In other words, neutrinos have three discrete masses but they do not correspond to three flavours. A neutrino flavour state can be considered as quantum superposition of all mass states or mass eigenstates.

During an experiment neutrinos produced via weak interaction are sent to detector placed at a distance. Neutrinos are emitted and absorbed as flavour states but travel as mass eigenstates. During the flight, three mass states will accumulate a quantum mechanical phase. The phase accumulated depends upon the mass of the state (will discuss it later). When neutrinos reach detector, these mass states

interfere producing a neutrino of particular flavour. The neutrino produced at the detector need not be same flavour as that of source. For fixed value of neutrino beam energy, flavour state detected varies as a function of distance. That is, flavour of neutrino at the detector depends only on the distance between source and detector. This is phenomenon is called Neutrino oscillations.

As said before, a particular flavour state is superposition of mass states. Each mass state is characterised by a definite mass. If we take plane wave solutions for mass state, the phase accumulated by the mass state depends upon its mass (will be shown later). Then neutrino oscillation can be studied as interference of mass eigenstates. Thus the probability of detecting a particular flavour in a particular distance depends upon difference in the phase. These phase difference vary as function of distance and energy of the neutrino beam (will be shown later). As a result of this, as neutrinos travel, it will be the admixture of all three flavours. The probability of detecting a flavour can be found out. It is found to be depend in sinusoidal manner on the source-detector distance and energy of the beam. Mass differences between neutrino flavours are small of $\sim 10^{-3}$ eV. As a result coherence length will be very high. Thus this microscopic quantum effect becomes observable over macroscopic distances.

Pontecorvo-Maki-Nakagawa-Sakata over the course of 10 years studied neutrino oscillation in vacuum in detail. They found that in an ultra relativistic scenario, the composition of the flavour state is given the PMNS matrix. But in 1985 Mikheyev and Smirnov modified the theory of neutrino oscillation to include matter effects on neutrino oscillation. Initial work in this direction was done by Wolfenstein in 1978. This effect is thus called Mikheyev Smirnov Wolfenstein effect (MSW effect).

2.1 Neutrino Flavour Oscillation in Vacuum

A neutrino source produces a neutrino along with a charged lepton. Flavour of the lepton (e, μ , or τ) produced would give us the flavour of neutrino produced (ν_e, ν_μ , or ν_τ). A neutrino created in a specific flavour eigenstate would be superposition of all three mass eigenstates. Experimentally, we can only detect the flavour state of neutrino. The relationship between flavour and mass states is encoded in the PMNS (Pontecorvo Maki Nakagawa Sakata) matrix. It is a unitary mixing matrix that contains information on the mismatch of quantum states of neutrinos when they propagate freely and when they take part in the weak interactions. Experiments have established values for the elements of this matrix [33].

Experimentally, a neutrino beam of known flux and flavour α is produced along with lepton l_α at the source. It is then send to a detector placed at a distance L from the source. There it would interact with the detector material to produce a secondary lepton l_β and neutrino ν_β . Thus at the time of interaction (with detector material), the neutrino would in β flavour (ν_β). One could detect the flavour change in two ways. One way is observe the appearance of neutrinos of new flavour β that is different from the original flavour ($\beta \neq \alpha$). Such type of experiments are called appearance experiments and would give us the appearance probability. The other way to is to look for the known flavour ν_α . There we measure the amount of flux disappeared compared to the initial beam. Such type of experiments are called disappearance experiments and would give us the disappearance probability or survival probability.

2.1.1 Theory of Flavour Oscillation

In order to explain the phenomenon of oscillations, one has to decompose a flavour eigenstate $|\nu_\alpha\rangle$ in the mass eigenstate basis $|\nu_i\rangle$. In a simple sense mass eigenstates are the eigenstates of the hamiltonian. Flavour states ($|\nu_e\rangle$, $|\nu_\mu\rangle$, $|\nu_\tau\rangle$) are not eigenstates of the hamiltonian and thus do not have definite energy eigenvalue. A mass eigenstate of type i with momentum p_i is an energy eigenstate with eigenvalues $E_i = \sqrt{p_i^2 + m_i^2}$ (in natural units). Flavour and mass eigenstates are connected via PMNS Matrix which is unitary. The matrix equation connecting flavour and mass states are given by:

$$\begin{bmatrix} |\nu_e\rangle \\ |\nu_\mu\rangle \\ |\nu_\tau\rangle \end{bmatrix} = \begin{bmatrix} U_{e1} & U_{e2} & U_{e3} \\ U_{\mu 1} & U_{\mu 2} & U_{\mu 3} \\ U_{\tau 1} & U_{\tau 2} & U_{\tau 3} \end{bmatrix} \begin{bmatrix} |\nu_1\rangle \\ |\nu_2\rangle \\ |\nu_3\rangle \end{bmatrix} \quad (2.1)$$

Thus a flavour state α can be written as a superposition of mass eigenstate.

$$|\nu_\alpha\rangle = \sum_{i=1,2,3} U_{\alpha i}^\dagger |\nu_i\rangle \quad (2.2)$$

Where $\alpha = e, \mu, \tau$ and quantities may be collected into a matrix known as PMNS matrix or leptonic mixing matrix. According to Standard Model U must be unitary. The relation connecting a particular flavour state to mass eigenstate can be inverted to express a mass eigenstate in terms of flavour state.

$$|\nu_i\rangle = \sum_{\alpha=e,\mu,\tau} U_{\alpha i} |\nu_\alpha\rangle \quad (2.3)$$

Where $|U_{\alpha i}|^2$ the probability that ν_i interacts with a detector to produce a charged lepton of the flavour of α . When standard three flavour oscillation is considered the

PMNS matrix is 3×3 in nature and for two flavour oscillation, it is 2×2 . It is given by

$$U = \begin{bmatrix} C_{12}C_{13} & S_{12}C_{13} & S_{13}e^{-i\delta} \\ S_{12}C_{23} - C_{12}C_{23}S_{13}e^{i\delta} & S_{12}C_{23} - S_{12}S_{23}S_{13}e^{i\delta} & S_{23}C_{13} \\ S_{12}S_{23} - C_{12}C_{23}S_{13}e^{i\delta} & -C_{12}S_{23} - S_{12}C_{23}S_{13}e^{i\delta} & C_{23}C_{13} \end{bmatrix} \begin{bmatrix} e^{\frac{i\alpha_1}{2}} & 0 & 0 \\ 0 & e^{\frac{i\alpha_2}{2}} & 0 \\ 0 & 0 & 0 \end{bmatrix} \quad (2.4)$$

Where $C_{ij} = \cos \theta_{ij}$, $S_{ij} = \sin \theta_{ij}$. The phase factors α_1 and α_2 (Majorana phases) are physically meaningful only if neutrinos are Majorana particles (i.e. if the neutrino is identical to its antineutrino) and do not enter into oscillation phenomena regardless. The phase factor δ known as the Dirac phase is non-zero only if neutrino oscillation violates CP symmetry, this has not yet have been experimentally observed. So in our discussion for convenience, we take δ and α_i to be zero. In the presence of an additional neutrino, the PMNS matrix gets modified into a 4×4 matrix. Such a neutrino is called sterile neutrino. The existence of such a neutrino flavour is not yet confirmed. But there are hints of its existence. Results from Daya Bay reactor experiment and MiniBooNE sheds light on its existence [34][35]

For simplicity, we first discuss two flavour neutrino oscillation even though all 3 neutrinos take part in neutrino oscillation. But two neutrino oscillation is a fairly accurate description in a number of experiments. For example, $\nu_\mu \rightarrow \nu_\tau$ transitions are relevant for atmospheric neutrinos, $\nu_e \rightarrow \nu_\alpha$ in solar neutrinos, $\nu_e \rightarrow \nu_\mu$ at reactor experiments and $\nu_\mu \rightarrow \nu_e$ at accelerator experiments [21].

Suppose we generate a neutrino beam containing a flavour state α . We send the neutrino beam along the x-axis and let them propagate in a free space towards a detector some distance L . Then mass eigenstates propagate according to the time-dependent Schrodinger equation with no potentials.

$$i \frac{d|\nu_i(t)\rangle}{dt} = E_i |\nu_i(t)\rangle \quad (2.5)$$

Here quantities are expressed in natural units ($c = 1 = \hbar$). Since $L = ct$, in natural units it would become $L = t$. E_i is the energy corresponding to the mass eigenstate ν_i .

The solution of this equation is a plane-wave :

$$|\nu_i(t)\rangle = e^{-i\phi_i} |\nu_i(0)\rangle \quad (2.6)$$

Where ϕ_i is the phase factor picked up by neutrino during propagation.

At some later time t the flavour state α will be :

$$|\nu_\alpha(t)\rangle = \sum_{i=1,2} U_{\alpha i}^\dagger e^{-i\phi_i} |\nu_i(0)\rangle \quad (2.7)$$

Inverting the mixing matrix we can write ;

$$|\nu_i(0)\rangle = \sum_{\gamma} U_{\gamma i} |\nu_{\gamma}(0)\rangle \quad (2.8)$$

Substituting equation (2.8) in equation (2.7), we can write the flavour state as

$$\begin{aligned} |\nu_{\alpha}(t)\rangle &= \sum_{i=1,2} U_{\alpha i}^{\dagger} e^{-i\phi_i} |\nu_i(0)\rangle \sum_{\gamma} U_{\gamma i} |\nu_{\gamma}(0)\rangle \\ &= \sum_i \sum_{\gamma} U_{\alpha i}^{\dagger} e^{-i\phi_i} U_{\gamma i} |\nu_{\gamma}(0)\rangle \end{aligned}$$

Thus the amplitude of a detecting a neutrino flavour β at a spacetime (L, t) given by,

$$\begin{aligned} A(\nu_{\alpha}(0) \rightarrow \nu_{\beta}(0)) &= \langle \nu_{\beta}(t) | \nu_{\alpha}(0) \rangle \\ &= \sum_{\gamma} \sum_i U_{\gamma i} e^{i\phi_i} U_{\beta i}^{\dagger} \langle \nu_{\gamma}(0) | \nu_{\alpha}(0) \rangle \\ &= \sum_k U_{\alpha i}^{\dagger} e^{i\phi_i} U_{\beta i} \end{aligned} \quad (2.9)$$

Where last step comes from the orthogonality of flavour state $\langle \nu_{\gamma}(0) | \nu_{\alpha}(0) \rangle = \delta_{\gamma\alpha}$. The oscillation probability is given by :

$$\begin{aligned} P(\nu_{\beta} \rightarrow \nu_{\alpha}) &= |A(\nu_{\beta}(0) \rightarrow \nu_{\alpha}(t))|^2 \\ &= \left| \sum_i U_{\alpha i}^{\dagger} e^{i\phi_i} U_{\beta i} \right|^2 \\ &= \sum_i \sum_j U_{\alpha i} U_{\beta i}^{\dagger} U_{\alpha j}^{\dagger} U_{\beta j} e^{-i(\phi_j - \phi_i)} \end{aligned} \quad (2.10)$$

For two flavour oscillation, U would be a 2×2 rotation matrix. The rotation matrix would rotate a vector in the flavour basis into a vector in the mass basis and vice versa.

$$U^{\dagger} = \begin{bmatrix} \cos \theta & -\sin \theta \\ \sin \theta & \cos \theta \end{bmatrix} \quad (2.11)$$

So that,

$$\begin{bmatrix} |\nu_{\alpha}\rangle \\ |\nu_{\beta}\rangle \end{bmatrix} = \begin{bmatrix} \cos \theta & -\sin \theta \\ \sin \theta & \cos \theta \end{bmatrix} \begin{bmatrix} |\nu_i\rangle \\ |\nu_j\rangle \end{bmatrix} \quad (2.12)$$

Where θ is called the mixing angle. It gives how flavour state is different from mass states. if $\theta = 0$ the mass states and flavour states exactly coincides. The value of θ is determined through experiments.

The form of U is substituted in the equation (2.10). On reduction, we could arrive at an equation of oscillation probability in terms of mixing angle and ϕ as:

$$P(\nu_{\alpha} \rightarrow \nu_{\beta}) = \sin^2(2\theta) \sin^2\left(\frac{\phi_i - \phi_j}{2}\right) \quad (2.13)$$

In lab frame, since assumed to be plane waves ϕ_i can be written as ;

$$\phi_i = E_i t - p_i x \quad (2.14)$$

To proceed further, we make a shady approximation. Usually, we assume the mass eigenstates either created with the same momentum or with the same energy. Since neutrino flavour is measured by observing charged leptons which is Lorentz invariant, the oscillation probability must be Lorentz invariant. But the relativistic transformation of energy and momentum implies that the equal momentum assumption cannot hold in different inertial frames [36]. Thus one has to assume all E_i 's as equal [37][38][39]. Otherway to put it is that only components in the neutrino beam having the same energy contribute coherently to a neutrino oscillation signal. The fact we need to make such an approximation come from our modelling of neutrino mass eigenstates as plane waves. If we model neutrino mass eigenstates as wave packets, we need not make any approximation and get the same results. But the mathematical treatment of such a model is never so easy [40][41][42]. Nevertheless, it has been found out that wave packet description is unnecessary while dealing with stationary sources. For stationary systems, all information necessary for single particle measurements is contained in the energy spectrum; and the sun or the reactor or even a supernova for most purposes can certain only be regarded as essentially stationary sources [37].

At energy E_i , mass eigenstate $|\nu_i\rangle$ of mass m_i have momentum in the ultra relativistic limit.

$$p_i = \sqrt{E^2 - m_i^2} \cong E - \frac{m_i^2}{2E} \quad (2.15)$$

The expression $E = m^2 c^4 + p^2 c^2$ gives the relativistic energy of a particle with rest mass m and momentum p . In the ultra-relativistic limit, energy would be almost completely contributed by the momentum part ($p^2 c^2 \gg mc^2$) and thus can be approximated by $E \approx pc$. In equation (2.15) we have used the fact that $m_i^2 \ll E^2$ in ultra-relativistic limit. Thus,

$$\phi_i \cong E(t - L) + \frac{m_i^2 L}{2E} \quad (2.16)$$

Where L is the distance of separation between the source and the detector.

In the equation (2.16), the term $E(t - L)$ act as a global phase (same for all mass eigenstates) and hence can be treated as irrelevant as no interesting physics happens with it. Thus equation (2.16) becomes :

$$\phi_i = \frac{m_i^2 L}{2E} \quad (2.17)$$

Substituting equation (2.17) in equation (2.6) we would get that,

$$|\nu_i(t)\rangle = e^{-\frac{im_i^2 L}{2E}} |\nu_i(0)\rangle \quad (2.18)$$

As propagating, the mass eigenstates gain a quantum mechanical phase which depends upon the m_i and L (For constant E). Since the mass eigenstates are combinations of flavour eigenstates, they interfere with the corresponding flavour components of each mass eigenstate. Constructive interference causes it to be possible to observe a neutrino created with a given flavour to change its flavour during its propagation. The probability of a neutrino oscillates to another flavour (termed as ‘Appearance probability’) is given by the equation (2.13). Then,

$$\phi_j - \phi_i = \frac{m_j^2}{2E} - \frac{m_i^2}{2E} = \frac{\Delta m^2 L}{2E} \quad (2.19)$$

Where $\Delta m^2 = m_j^2 - m_i^2$. Substituting back into equation (2.13) we get

$$P(\nu_\alpha \rightarrow \nu_\beta) = \sin^2(2\theta) \sin^2\left(\frac{\Delta m^2 L}{4E}\right) \quad (2.20)$$

If we agree to measure L in units of kilometres and E in GeV and put back \hbar and c which was earlier left out into equation (2.20),

$$\begin{aligned} P(\nu_\alpha \rightarrow \nu_\beta) &= \sin^2(2\theta) \sin^2\left(\frac{\Delta m^2 c^3 L}{4\hbar E}\right) \\ P(\nu_\alpha \rightarrow \nu_\beta) &= \sin^2(2\theta) \sin^2\left(1.27 \frac{\Delta m^2 L}{E}\right) \end{aligned}$$

The corresponding survival probability (or disappearance probability) that is generating an α flavour neutrino and detecting the same flavoured neutrino is given by,

$$P(\nu_\alpha \rightarrow \nu_\alpha) = 1 - \sin^2(2\theta) \sin^2\left(1.27 \frac{\Delta m^2 L}{E}\right) \quad (2.21)$$

The same mathematical treatment can be used in the case of three flavour to develop theory of three flavour oscillation. Using the equation (2.2), we can write ν_α at $t = 0$ as;

$$|\nu_\alpha(0)\rangle = U_{\alpha 1}^\dagger |\nu_1\rangle + U_{\alpha 2}^\dagger |\nu_2\rangle + U_{\alpha 3}^\dagger |\nu_3\rangle \quad (2.22)$$

After travelling a distance of L the state of the state of neutrino would be (given by equation (2.6)),

$$|\nu_\alpha(t)\rangle = U_{\alpha 1}^\dagger e^{i\phi_1} |\nu_1\rangle + U_{\alpha 2}^\dagger e^{i\phi_2} |\nu_2\rangle + U_{\alpha 3}^\dagger e^{i\phi_3} |\nu_3\rangle \quad (2.23)$$

Where $\phi_i = E_i t - p_i x$. For a detector placed at distance L from the source, in the ultra-relativistic limit, $\phi_i \cong \frac{m_i^2 L}{2E_i}$. Thus state evolution can be expressed in terms of L alone.

Expressing the mass eigenstates in terms of the flavour eigenstates in equation (2.23),

$$\begin{aligned} |\nu_\alpha(t)\rangle &= (U_{\alpha 1}^\dagger U_{e1} e^{-i\phi_1} + U_{\alpha 2}^\dagger U_{e2} e^{-i\phi_2} + U_{\alpha 3}^\dagger U_{e3} e^{-i\phi_3}) |\nu_e\rangle \\ &\quad + (U_{\alpha 1}^\dagger U_{\mu 1} e^{-i\phi_1} + U_{\alpha 2}^\dagger U_{\mu 2} e^{-i\phi_2} + U_{\alpha 3}^\dagger U_{\mu 3} e^{-i\phi_3}) |\nu_\mu\rangle \\ &\quad + (U_{\alpha 1}^\dagger U_{\tau 1} e^{-i\phi_1} + U_{\alpha 2}^\dagger U_{\tau 2} e^{-i\phi_2} + U_{\alpha 3}^\dagger U_{\tau 3} e^{-i\phi_3}) |\nu_\tau\rangle \end{aligned} \quad (2.24)$$

Thus oscillation probability $P(\nu_\alpha \rightarrow \nu_\beta)$ is given by,

$$\begin{aligned} P(\nu_\alpha \rightarrow \nu_\beta) &= |\langle \nu_\beta | \nu_\alpha \rangle|^2 \\ &= |U_{\alpha 1}^\dagger U_{\beta 1} e^{-i\phi_1} + U_{\alpha 2}^\dagger U_{\beta 2} e^{-i\phi_2} + U_{\alpha 3}^\dagger U_{\beta 3} e^{-i\phi_3}|^2 \end{aligned} \quad (2.25)$$

On solving equation (2.25) we could derive a form for $P(\nu_\alpha \rightarrow \nu_\beta)$ as

$$P(\nu_\alpha \rightarrow \nu_\beta) = \delta_{\alpha\beta} - 4 \sum_{i>j} (U_{\alpha i} U_{\beta i} U_{\alpha j} U_{\beta j}) \sin^2(\Delta m_{ij}^2 \frac{L}{4E}) \quad (2.26)$$

While solving equation 2.25 we assume that the Dirac phase $\delta = 0$ that is there is no charge parity violation.

Let us consider an appearance experiment ($\alpha \neq \beta$). Then,

$$\begin{aligned} P(\nu_\alpha \rightarrow \nu_\beta) &= -4 \sum_{i>j} (U_{\alpha i} U_{\beta i} U_{\alpha j} U_{\beta j}) \sin^2(1.27 \frac{\Delta m_{ij}^2 L}{E}) \\ &= -4[(U_{\alpha 1} U_{\beta 1} U_{\alpha 2} U_{\beta 2}) \sin^2(1.27 \frac{\Delta m_{12}^2 L}{E}) \\ &\quad + (U_{\alpha 1} U_{\beta 1} U_{\alpha 3} U_{\beta 3}) \sin^2(1.27 \frac{\Delta m_{13}^2 L}{E}) \\ &\quad + (U_{\alpha 2} U_{\beta 2} U_{\alpha 3} U_{\beta 3}) \sin^2(1.27 \frac{\Delta m_{23}^2 L}{E})] \end{aligned} \quad (2.27)$$

Since there are three mass states there would be two independent mass splittings, called Δm_{23}^2 and Δm_{12}^2 . The other splitting is defined by the relation $\Delta m_{12}^2 + \Delta m_{23}^2 + \Delta m_{13}^2 = 0$. From solar and atmospheric neutrino problems it is measured that $\Delta m_{12}^2 \sim 10^{-5} eV^2$ and $\Delta m_{23}^2 \sim 10^{-3} eV^2$. Thus at reasonable approximation $\Delta m_{23}^2 \approx \Delta m_{13}^2$ at low $\frac{L}{E}$ limit we can approximate equation (2.27) as

$$P(\nu_\alpha \rightarrow \nu_\beta) = -4[U_{\alpha 1} U_{\beta 1} U_{\alpha 3} U_{\beta 3} + U_{\alpha 2} U_{\beta 2} U_{\alpha 3} U_{\beta 3}] \sin^2(\frac{1.27 \Delta m_{23}^2 L}{E}) \quad (2.28)$$

Through experiments we can determine the mixing angle (θ_{ij}) and mass splittings (Δm_{ij}). By substituting it into the matrix given by the equation (2.4) we can find out PMNS matrix (assume $\delta, \alpha = 0$). Substituting the matrix elements back into equation (4.1) would give probability neutrino of a particular flavour to oscillate at a distance L from the source.

Chapter 3

Entanglement in Neutrino Oscillations

Quantum entanglement, one can describe it as the most non-classical illustration of the quantum formalism. The term 'Entanglement' was coined by Schrödinger, originally called it as 'Verschränkung' (German). It underlines the inherent correlation between subsystems of a compound quantum system. This holistic property of the compound system has proven to be useful in a wide range of applications. Quantum teleportation, quantum dense coding, quantum cryptography, quantum computations etc are some of the key areas where entanglement is exploited. A formal definition for entanglement is provided by Horodecki *et al.*(2007), "*This feature (entanglement) implies the existence of global states of quantum systems which cannot be written as a product of states of individual subsystems*". Now, this definition does not look terrifying as it should be. But this particular phenomenon has baffled numerous scientist including Einstein. Entanglement violated *The Principle of Locality* and *The principle of Realism* [43], two cornerstones of the classical physics. This disturbed Einstein and he referred entanglement as *spooky action at a distance*.

During early the times of quantum mechanics, to save the Goliath ("Classical Physics") from the David ("Entanglement"), Einstein-Podolsky-Rosen put forward Local Hidden Variable Model (LHVM) [44] to explain entanglement. According LHVM, quantum mechanics was an incomplete theory. It was proposed that quantum mechanics can be completed by introducing the so-called *Hidden Variables*. Thus the proposal was that measurement is a deterministic process and it appears probabilistic only because some degrees of freedom are not known (Hidden Variables). But as like the story of David and Goliath, against all odds entanglement emerged as the victor in the scientific conflict that span over three decades. Bell published his famous paper named "*On The Einstein Podolsky Rosen Paradox*" [45]

in 1964. In this paper, Bell accepted LHV Model and formulated a set of inequalities that the system need to obey to conserve principles of locality and realism. This later came to be known as Bell's theorem. But in 1981 – 82 using entangled photons, Aspect *et al.* performed convincing tests which showed the violation of Bell's Inequalities (Bell's Theorem) [46][47]. Numerous experiments were conducted before and after this, all of these agreed with the predictions of quantum formalism.

3.1 Single Particle Entanglement

It was believed that a minimum of two particles was necessary for the system to exhibit entanglement. Thus the state represented by the equation (3.1) cannot have entanglement.

$$|\psi\rangle_{AB} = c_1 |1\rangle_A |0\rangle_B + c_2 |0\rangle_A |1\rangle_B \quad (3.1)$$

Where, $\sum_i c_i^2 = 1$ and $|0\rangle_{A,B}$ and $|1\rangle_{A,B}$ represent state with zero and one particle, respectively, in mode A and B . To get a physical picture, consider the particles to be photons i.e. $|0\rangle$ and $|1\rangle$ are the Fock states (number state) of photons. If we consider A and B as the Horizontal and Vertical polarization, then state (3.1) represent a diagonally polarized photon. Normally such states are not regarded as entangled.

But van Enk showed that such single-particle states can do have entanglement, provided two modes A and B are spatially separated [25]. He showed that (theoretically), a two particle entangled state can be constructed from the state (3.1) employing only local operations. But according to quantum information theory, between two distant systems entanglement cannot be created (or increased) through local operations [48][49]. Thus it would not be possible to create entanglement through local operations. However, this restriction still allows one to transform entanglement in a system into entanglement involving other systems [50]. This would eventually lead to the conclusion that state (3.1) is entangled.

Often reader may get mislead when we say that state (3.1) is entangled. One may tend to believe that entanglement is between the particle and the vacuum state ($|0\rangle$). But this is not true. The entanglement is between the spatially separated modes A and B . So in the case of single photons, entanglement is not between the photon and vacuum but between different modes (e.g. Horizontal and Vertical polarization). Further, there are **proposals such states have used** to perform quantum cryptography, teleportation and to check the violation of Bell's inequalities etc. [51][52][53]. This confirms the existence of single-particle entanglement. Thus for entanglement to be well-defined **one only needs** two Hilbert spaces (degree of freedom), not two

particles. In the case of the second quantized field, particle number is a valid degree of freedom. For such a field, one can have two Hilbert spaces corresponding to two spatially separated modes (like the state (3.1)).

3.2 Entanglement in Neutrinos

In the section (2.1), we discussed the theory of neutrino flavour oscillation in a vacuum. And we found that the flavour state of a neutrino can be written as a coherent superposition of mass states.

$$|\nu_\alpha\rangle = \sum_{i=1,2,3} U_{\alpha i}^\dagger |\nu_i\rangle \quad (3.2)$$

Where $\alpha = e, \mu, \tau$ and U is called the PMNS matrix, it is given by the equation (2.4). Throughout the discussion, we are taking the Dirac phase $\delta = 0$ and Majorana phase $\alpha = 0$. Also note that, $\langle \nu_\alpha | \nu_\beta \rangle = \delta_{\alpha\beta}$ and $\langle \nu_i | \nu_j \rangle = \delta_{ij}$.

Neutrino flavour oscillations happens due to neutrino mixing and neutrino mass difference. The neutrino state $|\nu_i\rangle$ is characterised by definite mass m_i and energy E_i . The propagation of neutrino states are given by plane wave solutions.

$$|\nu_i(t)\rangle = \exp(-iE_i t) |\nu(0)\rangle$$

The time evolution of neutrino flavour state is given by,

$$|\nu_\alpha(t)\rangle = \tilde{U}(t) |\nu_\alpha(0)\rangle \quad (3.3)$$

Where $\tilde{U}(t) \equiv U_{PMNS} U_0(t) U_{PMNS}^\dagger$. The time evolution of mass states are given by the matrix

$$U_0(t) = \text{diag}[e^{-iE_1 t}, e^{-iE_2 t}, e^{-iE_3 t}]$$

Then at time t , the transition probability for $\nu_\alpha \rightarrow \nu_\beta$ is,

$$P_{\nu_\alpha \rightarrow \nu_\beta}(t) = |\langle \nu_\beta | \nu_\alpha(t) \rangle|^2 = |\tilde{U}_{\alpha\beta}(t)|^2 \quad (3.4)$$

Where $\alpha, \beta = e, \mu, \tau$. In the ultra-relativistic limits, transition probability $P_{\nu_\alpha \rightarrow \nu_\beta}(t)$ is a function baseline (L) and Energy of the neutrino beam (E).

In the above framework, one can discuss entanglement in neutrinos by mapping neutrino flavour states into three-qubit states. Thus flavour states can be written as,

$$\begin{aligned} |\nu_e\rangle &\equiv |1\rangle_{\nu_e} |0\rangle_{\nu_\mu} |0\rangle_{\nu_\tau} \\ |\nu_\mu\rangle &\equiv |0\rangle_{\nu_e} |1\rangle_{\nu_\mu} |0\rangle_{\nu_\tau} \\ |\nu_\tau\rangle &\equiv |0\rangle_{\nu_e} |0\rangle_{\nu_\mu} |1\rangle_{\nu_\tau} \end{aligned} \quad (3.5)$$

Where states $|0\rangle_{\nu_\alpha}$ and $|1\rangle_{\nu_\alpha}$ correspond to the presence and absence of a neutrino in a mode α . Thus we can recast the equation (3.3) as,

$$|\nu_\alpha(t)\rangle = \tilde{\mathbf{U}}_{\alpha e}(t)|1\rangle_{\nu_e}|0\rangle_{\nu_\mu}|0\rangle_{\nu_\tau} + \tilde{\mathbf{U}}_{\alpha \mu}(t)|0\rangle_{\nu_e}|1\rangle_{\nu_\mu}|0\rangle_{\nu_\tau} + \tilde{\mathbf{U}}_{\alpha \tau}(t)|0\rangle_{\nu_e}|0\rangle_{\nu_\mu}|1\rangle_{\nu_\tau} \quad (3.6)$$

Where $\sum_\beta |\tilde{\mathbf{U}}_{\alpha e}(t)|^2 = 1$ and $\alpha, \beta = e, \mu, \tau$.

The state $|\nu_\alpha(t)\rangle$ is not bi-seperable. A state $|\psi\rangle$ composed of N particles is said to be bi-seperable, if we can write $|\psi\rangle = |\phi\rangle_A \otimes |\gamma\rangle_B$, where A and B are two sub-partition of the system and $A \cup B = N$. Thus the equation (3.6) represent an entangled state. It belong to the class of W-states. They (W-states) are maximally entangled tripartite states of the form,

$$|\psi\rangle = \frac{1}{\sqrt{3}}[|100\rangle + |010\rangle + |001\rangle] \quad (3.7)$$

In short, $|\nu_\alpha(t)\rangle$ is an entangled superposition of three-flavour states with time dependent coefficients.

Now consider the two-flavour case. Let the system be an electron-muon neutrino system i.e. tau does not takes place in oscillation. Then we can write $|\nu_\alpha(t)\rangle$ as,

$$|\nu_\alpha(t)\rangle = \tilde{\mathbf{U}}_{\alpha e}(t)|1\rangle_{\nu_e}|0\rangle_{\nu_\mu} + \tilde{\mathbf{U}}_{\alpha \mu}(t)|0\rangle_{\nu_e}|1\rangle_{\nu_\mu} \quad (3.8)$$

Where $\alpha = e, \mu$. We consider this particular system since it would be useful in later part.

3.3 Entaglement Measurement

3.3.1 Pure and Mixed States

The state $|\nu_\alpha(t)\rangle$ is a pure state. Now, in quantum mechanics, depending upon the information accessible about the system, we can classify the state of the system as ‘Pure’ and ‘Mixed’ state. If we have complete information of the system, then we call the state a Pure state. One can give another definition for the pure state as the state which cannot be written as the statistical mixture of other states. A pure state is of the form,

$$|\psi(t)\rangle = \sum_n c_n(t)|\phi_n\rangle \quad (3.9)$$

Where $\sum_n |c_n|^2 = 1$. The states we discussed till now belong this class. The time evolution of these states are governed by the Schrodinger equation,

$$i\hbar \frac{d}{dt}|\psi\rangle = \hat{H}|\psi\rangle \quad (3.10)$$

Now, we use a mixed state to represent a system state when we only know that state is taken from the ensemble of pure state

$$\{|\psi_1\rangle, |\psi_2\rangle, \dots, |\psi_l\rangle\} \quad (3.11)$$

Each pure state $|\psi_k\rangle$ occur with probability p_k and satisfying $\sum_k p_k = 1$. In short, we use a mixed state when system information is incomplete. In such a case, the state of system is given by the density matrix.

$$\rho = \sum_k p_k |\psi_k\rangle \langle \psi_k| \quad (3.12)$$

The evolution of mixed states is governed by the Liouville equation.

$$\frac{d\rho}{dt} = -i[H, \rho] \quad (3.13)$$

In similar manner, we can write the density matrix of a pure state $|\psi\rangle$ also. It is given by,

$$\rho = |\psi\rangle \langle \psi| \quad (3.14)$$

Schmidt decomposition

Consider a general quantum system. Let the system consist of two parts A and B (bi-partite system). Then any pure state $|\Psi\rangle$ can be written as :

$$|\Psi\rangle = \sum_{i=1}^n c_i |\psi_i^A\rangle |\psi_i^B\rangle \quad (3.15)$$

where $\{|\psi_1^A\rangle, |\psi_2^A\rangle, \dots, |\psi_n^A\rangle\}$ and $\{|\psi_1^B\rangle, |\psi_2^B\rangle, \dots, |\psi_n^B\rangle\}$ are set of orthonormal states for the subsystem A and B and the c_i 's are positive numbers. The number of non zero terms in the summation (3.3.1) is called the Schmidt number. It act as criteria for Entangled and seperable pure states.

1. If the Schmidt number < 1 , the system will be a separable pure state.
2. If the Schmidt number > 1 , the system will be an entangled pure state.

Now, c_i is called called Schmidt coefficients. Similarly, $|\psi_i^A\rangle$ and $|\psi_i^B\rangle$ are called Schmidt bases.

Pure and Mixed entangled state

For any composite system, a pure state is said to be entangled if the parts of the system are not pure states [54]. That is, the whole system will be a pure state, but the individual subsystems will be mixed states. This property arises as a consequence of entanglement. When two systems get entangled, we cannot specify the state of a single system alone. The state of one system depends on the other system and vice versa. Similarly, one can define the concept of entanglement for mixed quantum states also. A mixed state is entangled if it cannot be represented as a mixture of unentangled pure states

3.4 Entanglement Entropy

In the later section, we saw how entanglement is related to the mixedness of the subsystems. Exploiting this feature of the entangled system, we can define a measure for entanglement. For bi-partite systems that are in a pure state, a single widely accepted measurement is the Entropy of the Entanglement. But for mixed states, there is no unique measurement. The three most common measurements used in the case of mixed states are Entanglement of formation, Distillable entanglement, Relative entropy of entanglement. One can construct numerous other types of measurement from these three.

In the case of the pure state, von Neumann entropy is the most adequate measurement of the entanglement [55]. Given the density matrix of a system to be ρ , the von Neumann entropy of the system is defined as,

$$S = -Tr(\rho \log \rho) \quad (3.16)$$

where "Tr" indicates Trace. The bi-partite von Neumann entropy is defined as the von Neumann entropy of the individual subsystems.

$$S(\rho_A) = -Tr(\rho_A \log \rho_A) = -Tr(\rho_B \log \rho_B) = S(\rho_B) \quad (3.17)$$

where, $\rho_A = Tr_B(\rho_{AB})$ and $\rho_B = Tr_A(\rho_{AB})$. Here ρ_A and ρ_B are the called the reduced density matrix of the composite system (ρ_{AB}). For a system in product state, individual subsystems would be pure state i.e, state of system can be written as tensor product of two pure state. Thus von Nuemann entropy of such system would be zero. For an entangled state, subsystems would be in a mixed state. Thus the von Neumann entropy would be non zero. In short,

1. If $S(\rho) = 0$, state of system would be Pure product state.

2. If $S(\rho) \neq 0$, state of system would be Pure entangled state.

3.5 Measurement of Entanglement in Neutrinos

Bipartite entanglement is quantified efficiently by von Neumann entropy. Also any monotonic functions of the former can itself act as a measure. Discussions about such entanglement monotones can be found in [56][57]. Linear entropy belong to this class of entanglement monotones. Linear entropy can be considered lower approximation to von Neumann entropy. The bipartite linear entropy S_L is defined as the linear entropy of the either of its reduced state (they can be shown equal). For system whose state represented by density matrix ρ , Linear entropy is defined as,

$$S_L = \frac{d}{d-1} (1 - \text{Tr}(\rho^2)) \quad (3.18)$$

More formal definition of linear entropy for a pure state $|\psi\rangle$ is as follows,

Consider a N -partite system $S = \{S_1, S_2, S_3, \dots, S_N\}$. Now let us bipartite the system in to two-subsystems S_A and S_B . Here $S_{A_n} = \{S_{i1}, S_{i2}, \dots, S_{in}\}$, with $1 \leq i_1 < i_2 < \dots < i_n \leq N$ ($1 \leq n < N$), and $S_{B_{N-n}} = \{S_{j1}, S_{j2}, \dots, S_{j(N-n)}\}$, with $1 \leq j_1 < j_2 < \dots < j_{N-n}$, and $i_q \neq j_p$. Let the density matrix of the system be $\rho_{AB} = |\psi\rangle\langle\psi|$. Then $\rho_{A_n} = \text{Tr}_{B_{N-n}}(\rho_{AB})$ denotes the reduced density matrix of subsystem S_{A_n} after tracing over subsystem $S_{B_{N-n}}$. The linear entropy of such a bi-partitioned system is defined as

$$S_L^{(A_n|B_{N-n})}(\rho_{AB}) = \frac{d}{d-1} (1 - \text{Tr}_{A_n}(\rho_{A_n}^2)) \quad (3.19)$$

where the d is the Hilbert-space dimension given by $d = \min[\dim S_{A_N}, \dim S_{B_{N-n}}] = \min[2^n, 2^{N-n}]$ [21].

We can also define average linear entropy as:

$$\langle S_L^{(n:N-n)}(\rho_{AB}) \rangle = \binom{N}{n}^{-1} \sum_{A_n} S_L^{(A_n;B_{N-n})}(\rho_{AB}) \quad (3.20)$$

The value of linear entropy varies between 0 to 1. For product state, value of linear entropy would be zero. For an entangled state, value of linear entropy would be non-zero. The state of the system will be maximally entangled if Linear entropy $S_L = 1$.

Linear Entropy of Neutrino

As mentioned in the previous section, the state $|\nu_\alpha(t)\rangle$ is a pure state. Thus we can use linear entropy to quantify the entanglement in the system. First consider two flavour case. Such a system shows bipartite entanglement. In particular we are taking electron-muon system (as they are used while simulation). For such a system, time evolved state is given by equation (3.8).

$$|\nu_\alpha(t)\rangle = \tilde{\mathbf{U}}_{\alpha e}(t)|1\rangle_{\nu_e}|0\rangle_{\nu_\mu} + \tilde{\mathbf{U}}_{\alpha \mu}(t)|0\rangle_{\nu_e}|1\rangle_{\nu_\mu} \quad (3.21)$$

where the coefficients $\tilde{\mathbf{U}}_{\alpha \beta}$ is given by the equation (3.4). For such a state, the density matrix will be $\rho_\alpha = |\nu_\alpha(t)\rangle \langle \nu_\alpha(t)|$. Using equation (3.19), we can straight forward calculate linear entropy by tracing over one of the modes.

$$\begin{aligned} S_{L\alpha}^{(e;\mu)} &= S_{L\alpha}^{(\mu;e)} = 4|\tilde{\mathbf{U}}_{\alpha e}(t)|^2|\tilde{\mathbf{U}}_{\alpha \mu}(t)|^2 \\ &= 4|\tilde{\mathbf{U}}_{\alpha e}(t)|^2(1 - |\tilde{\mathbf{U}}_{\alpha e}(t)|^2) \\ &= 4|\tilde{\mathbf{U}}_{\alpha \mu}(t)|^2(1 - |\tilde{\mathbf{U}}_{\alpha \mu}(t)|^2) \end{aligned} \quad (3.22)$$

where, $S_{L\alpha}^{(e;\mu)} \equiv S_L^{(e;\mu)}(\rho^{(\alpha)})$. Here α refers the time evolved channel and the superscripts $(e;\mu)$ refers to considered flavour modes (here it is electron and muon flavours).

As we move from two-flavour to three-flavour case, we deals with multipartite entanglement (more than 2 modes). Still we can quantify the entanglement using some bipartite measures. Global entanglement is such a measure. It is defined as the sum of all the bipartite entanglement between a single subsystem and each of the remaining ones. This can be expressed as average subsystem linear entropy. Thus it can be generalised as the sum of average linear entropies of all the possible bi-partitions of the system[57][58].

For three flavour oscillation, linear entropy is given by,

$$\begin{aligned} S_{L\alpha}^{(e,\mu;\tau)} &= 4|\tilde{\mathbf{U}}_{\alpha \tau}(t)|^2(|\tilde{\mathbf{U}}_{\alpha \mu}(t)|^2 + |\tilde{\mathbf{U}}_{\alpha e}(t)|^2) \\ S_{L\alpha}^{(e,\mu;\tau)} &= 4|\tilde{\mathbf{U}}_{\alpha \tau}(t)|^2(1 - |\tilde{\mathbf{U}}_{\alpha \tau}(t)|^2) \end{aligned} \quad (3.23)$$

Here tracing is done over mode τ and linear entropies of other bi-partitions can be obtained by permuting over the indices e,μ . They are,

$$\begin{aligned} S_{L\alpha}^{(\mu,\tau;e)} &= 4|\tilde{\mathbf{U}}_{\alpha e}(t)|^2(1 - |\tilde{\mathbf{U}}_{\alpha e}(t)|^2) \\ S_{L\alpha}^{(\tau,e;\mu)} &= 4|\tilde{\mathbf{U}}_{\alpha \mu}(t)|^2(1 - |\tilde{\mathbf{U}}_{\alpha \mu}(t)|^2) \end{aligned} \quad (3.24)$$

The average linear entropy in the three-flavour case is given by,

$$\langle S_{L\alpha}^{(2:1)} \rangle = \frac{8}{3}(|\tilde{\mathbf{U}}_{\alpha e}(t)|^2|\tilde{\mathbf{U}}_{\alpha \mu}(t)|^2 + |\tilde{\mathbf{U}}_{\alpha e}(t)|^2|\tilde{\mathbf{U}}_{\alpha \tau}(t)|^2 + |\tilde{\mathbf{U}}_{\alpha \mu}(t)|^2|\tilde{\mathbf{U}}_{\alpha \tau}(t)|^2) \quad (3.25)$$

The equation (3.25) gives us the global entanglement of the three-flavor system. Thus using linear entropy we can effectively quantify the entanglement in neutrino.

Chapter 4

Neutrino Oscillation in a quantum processor

The spontaneous transition of neutrino flavour over a macroscopic distance occurs due to the non-coinciding of flavour and mass eigenstates called Neutrino Oscillation. Neutrino oscillation through its periodic nature has given insights that neutrinos have non zero mass, which is something beyond the Standard Model's predictions. Thus neutrino oscillations indicate the existence of physics outside the standard model. Experimentally when we study neutrino oscillation what we do inspect the neutrino oscillation behaviour at different values of energies E and baseline L . For different $\frac{L}{E}$ values, we perform either appearance experiment (or disappearance experiment) and get appearance probability (or disappearance probability). Using experimentally obtained probabilities we would fix the values of the mixing angle (θ_{ij}) and squared mass difference (Δm_{ij}^2) by putting them back into the corresponding equation.

Experimental detection of neutrino oscillation would require sophisticated instruments. Often the labs are kept underground. This to prevent the interference due to cosmic rays. We cannot detect all flavours using single type of detector. Detectors depending upon the type, work at different energy range and threshold energy below which detection of neutrinos is not possible. For example, detectors using water as detector material, detect neutrinos via elastic scattering will not work for neutrinos of low energy ($< 5\text{MeV}$). Similarly, Chlorine-based detectors have a threshold of 0.814 MeV.

Another thing that often concerns the experimentalist is the sensitivity of the detectors. In the case of reactor-based or accelerator-based experiments sensitivity of the detector depends upon the baseline length. For e.g., for a neutrino beam of

energy $E \sim 1\text{GeV}$ detector baseline should be at least of the order of 10^4 for it to be sensitive to Δm_{ij}^2 down to $\sim 10^{-4}\text{eV}^2$. So we need to produce high energetic neutrino beams to reduce the baseline without compromising sensitivity. In such a scenario simulation studies aid us. Using the experimentally determined parameters, we can perform simulation studies of the flavour oscillation for neutrino beams of energies inaccessible under lab conditions.

Not so long after Feynman put forward the idea of simulating a quantum system with another, the possibility of using a quantum computer to simulate quantum systems was understood. The major difference between a classical computer and a quantum computer in simulating quantum systems is that the quantum computer performs actual Hamiltonian evolution whereas others just emulate it. At the present stage, even though the result got by quantum simulations is not praiseworthy as that of classical simulations, the computational cost of quantum algorithms are much less compared to classical algorithms for simulating a quantum system. The development of fault tolerant quantum computation would give us more reliable results enable us to manoeuvre the quantum advantage in a wide variety of fields.

Here we perform quantum simulation by executing an analogous Hamiltonian evolution to generate neutrino flavour oscillation. Such encoding and evolution is a stepping stone towards developing more advanced quantum simulations of neutrino oscillation. Systems that could particularly benefit from the quantum algorithmic approach to neutrino flavour evolution include those where collective neutrino oscillations are relevant, such as in Supernovae or the early Universe [1]. In such cases, the quantum Boltzmann equation which gives the evolution neutrino population can only be solved approximately.

In this section, we are going to first discuss how to encode two neutrino system evolution on a quantum computer using only a single qubit. Then we extend this idea to implement three flavour oscillation in a two qubit space inside a quantum processor. While simulating, the primary challenge that lies ahead is to implement the PMNS matrix which relates the flavour and mass eigenstates. Here we use the algorithm or the circuit put forward by Argüelles *et.al* 2019, to study neutrino flavour oscillation. This algorithm uses quantum gates to realise the PMNS matrix and to realise the time evolution operator. The algorithm is discussed below.

4.1 Simulation of Two Flavour Oscillation

In this circuit we only use a single qubit to encode neutrino flavour state and to time evolve the states we apply corresponding quantum gates. Let our system have of two neutrino flavour state let say α and β . Now we want to encode these states on qubits and encoding scheme we follow is given below.

$$|\nu_\alpha\rangle = \begin{bmatrix} 1 \\ 0 \end{bmatrix}, |\nu_\beta\rangle = \begin{bmatrix} 0 \\ 1 \end{bmatrix} \quad (4.1)$$

In the case of two flavour oscillation is the PMNS matrix is given by the 2x2 rotation matrix.

$$U = \begin{bmatrix} \cos \theta & \sin \theta \\ -\sin \theta & \cos \theta \end{bmatrix} \quad (4.2)$$

PMNS operation is encoded in IBM Quantum computer by three-parameter U gate. The matrix form of the gate is given as :

$$U(\Theta, \Phi, \Lambda) = \begin{bmatrix} \cos\left(\frac{\Theta}{2}\right) & -\sin\left(\frac{\Theta}{2}\right)e^{i\Lambda} \\ \sin\left(\frac{\Theta}{2}\right)e^{i\Phi} & \cos\left(\frac{\Theta}{2}\right)e^{i(\Lambda+\Phi)} \end{bmatrix} \quad (4.3)$$

For a two-neutrino system, the oscillation probabilities depend upon a single parameter known as mixing angle. Thus the U gate which having 3 parameters has to be modified,

1. Now consider the case of including the parameter Φ . This corresponds to the re-phasing of charged lepton field, and standard Lagrangian is invariant under such an operation. For e.g., let us consider the case of a muon neutrino. The presence of Φ corresponds to re-phasing $|\nu_\mu\rangle$ by $e^{-i\Phi} |\nu_\mu\rangle$. As said before, under such a transformation Lagrangian remains invariant and does not influence oscillation probabilities [59]. Thus we can take $\Phi = 0$ without loss of any generality.
2. We can use the same arguments provided above to set $\Lambda = 0$ for the case of Dirac fermions [59]. But this is not possible in the case of neutrino being a Majorana particle. For Majorana particle, this phase is physical and should be maintained in the Lagrangian. However, it is proven the presence of such a phase would not affect the oscillation probabilities [60] and thus can be taken equal to zero while studying the neutrino oscillation irrespective of the type of particle.

Thus using a U gate we can realise the PMNS matrix by suitably choosing the value of the parameters.

$$U_{PMNS}^{2 \times 2} = U(-2\theta, 0, 0) = \begin{bmatrix} \cos \theta & \sin \theta \\ -\sin \theta & \cos \theta \end{bmatrix} \quad (4.4)$$

Where θ is the mixing angle.

Using the PMNS matrix that we realised using U gate, flavour state encoded in the qubit equation (4.1) can be rotated into in the mass basis $\{|\nu_1\rangle, |\nu_2\rangle\}$. After rotating into mass basis we have to time evolve the mass states. From equation (2.7) we know that,

$$\begin{aligned} |\nu_\alpha(t)\rangle &= U_{\alpha 1}^\dagger e^{i\phi_1} |\nu_1\rangle + U_{\alpha 2}^\dagger e^{i\phi_2} |\nu_2\rangle \\ &= e^{i\phi_1} (U_{\alpha 1}^\dagger |\nu_1\rangle + U_{\alpha 2}^\dagger e^{i\Delta\phi} |\nu_2\rangle) \end{aligned}$$

Where $\Delta\phi = \phi = \phi_2 - \phi_1$. Global phases like $e^{i\phi_1}$ have no physical significance and can be discarded [43], relative phases between mass states are only relevant for neutrino oscillations, and without losing any generality we can measure all phases relative to $|\nu_1\rangle$ state. Thus time evolution operator can also be encoded by using a U gate.

$$\mathbf{U}(t) = U(0, 0, \phi) = \begin{bmatrix} 1 & 0 \\ 0 & e^{i\phi} \end{bmatrix} \quad (4.5)$$

Where $\phi = \frac{\Delta m^2 t}{2E}$ (equation (2.17-2.19)) in natural units and under ultra-relativistic approximation.

After time evolving the mass states it is rotated again back into flavour basis using applying U gates and is measured to get back the final state. Note that by simply changing parameter $\theta \rightarrow -\theta$ in the equation (4.4), U^\dagger can be constructed out of U gate.

$$U_{PMNS}^{2x2 \dagger} = U(2\theta, 0, 0) = \begin{bmatrix} \cos \theta & -\sin \theta \\ \sin \theta & \cos \theta \end{bmatrix} \quad (4.6)$$

4.2 Simulation of Three Flavour Neutrino Oscillation

Using only one qubit, we can only construct a Hilbert space of dimension two. A three flavour neutrino oscillation involves a dimension of 3 and requires more than

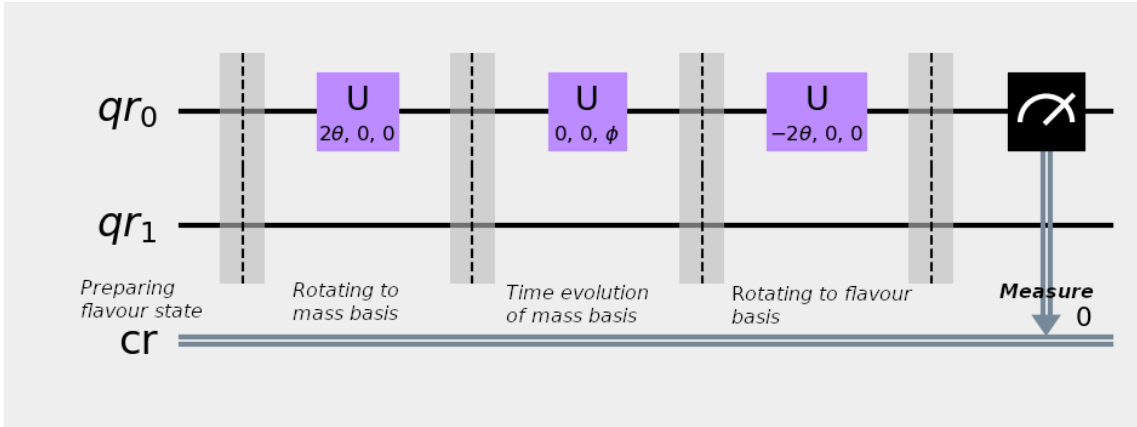


Figure 4.1: Circuit simulating two flavour oscillation[1]

one qubit. So three flavours of neutrino are encoded by using 2-qubits. The encoding scheme we follow is that,

$$\begin{aligned}
 |\nu_e\rangle = |00\rangle &= \begin{bmatrix} 1 \\ 0 \\ 0 \\ 0 \end{bmatrix}, \quad |\nu_\tau\rangle = |01\rangle = \begin{bmatrix} 0 \\ 1 \\ 0 \\ 0 \end{bmatrix} \\
 |\nu_\mu\rangle = |10\rangle &= \begin{bmatrix} 0 \\ 0 \\ 1 \\ 0 \end{bmatrix}, \quad |\nu_x\rangle = |01\rangle = \begin{bmatrix} 0 \\ 0 \\ 0 \\ 1 \end{bmatrix}
 \end{aligned} \tag{4.7}$$

There is one redundant basis state $|\nu_x\rangle$ in this encoding. This could represent the fourth flavour of neutrino in models with sterile neutrinos. But for our discussion, we consider it as physically decoupled and thus unphysical. The circuit is designed in such a way that fourth state does not take part in oscillation. Here also we follow the same methodology as discussed in the two flavour case. We prepare flavour states and do the unitary transformation of flavour state into mass basis, then time evolve the mass states and transform it back into flavour basis and measure it. Now, realising the PMNS matrix using quantum gates is not trivial as in the case of two flavour case. Here we follow the circuit proposed by Argüelles and jones (2019)[1], in which U gates and $CNOT$ gates are used for realising the PMNS matrix.

The above circuit is designed in such a way as to mimic the action of the PMNS matrix. To fix the free parameters on this circuit, the circuit is mapped onto a matrix multiplication on the computational basis. A numerical fit is then performed to match the experimentally determined PMNS matrix. The input values of the

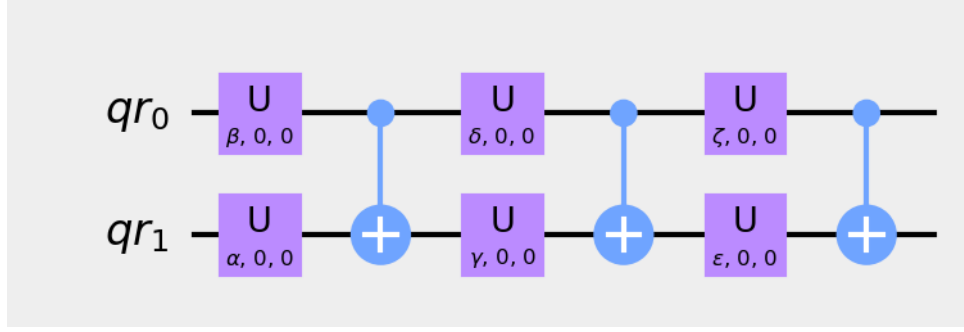


Figure 4.2: Gate arrangement for realizing PMNS matrix[1]

PMNS matrix used to fit the parameters are from [61] and are,

$$U_{PMNS} = \begin{bmatrix} 0.821427 & 0.550313 & 0.149708 & 0 \\ -0.481513 & 0.528538 & 0.699138 & 0 \\ 0.305618 & -0.646377 & 0.699138 & 0 \\ 0 & 0 & 0 & 1 \end{bmatrix} \quad (4.8)$$

Here we consider the PMNS matrix of 4×4 form since the encoding scheme uses 2-qubit which fhttps://www.overleaf.com/project/6098a408b10c8ee4104c10d2orms 4-dimensional Hilbert space. The last row represents decoupled physical state and will not take part in flavour oscillation.

The PMNS matrix is fitted by the method of gradient minimization over the six parameters (sum of squared residuals of each element of the matrix is minimised). The best fit parameter provided in [1] are,

$$\alpha = -0.6031, \beta = -2.0125, \gamma = -0.7966, \delta = 1.0139, \epsilon = 0.7053, \zeta = 1.3599 \quad (4.9)$$

Substitution of parameters given by the equation (4.9) in the circuit would give us PMNS matrix and $PMNS^\dagger$ is got by inverting the gate arrangement.

The evolution operation $\mathbf{U}(t)$ in computational basis is given by,

$$\mathbf{U}(t) = \exp[i \operatorname{diag}(0, \Delta m_{12}^2 \frac{t}{2E}, \Delta m_{13}^2 \frac{t}{2E}, \Phi)] \quad (4.10)$$

Where Φ is arbitrary phase that can be picked up for convenience and can be discarded since fourth basis state is not observable. Such a time evolution operator is realised using two U gates.

$$\mathbf{U}(t) = U(0, 0, \phi_1) \otimes U(0, 0, \phi_2) \quad (4.11)$$

Where $\phi_1 = \frac{\Delta m_{13}^2}{2E}$ and $\phi_2 = \frac{\Delta m_{12}^2}{2E}$.

The circuit for simulating three flavour oscillation is given in the figure 4.3.

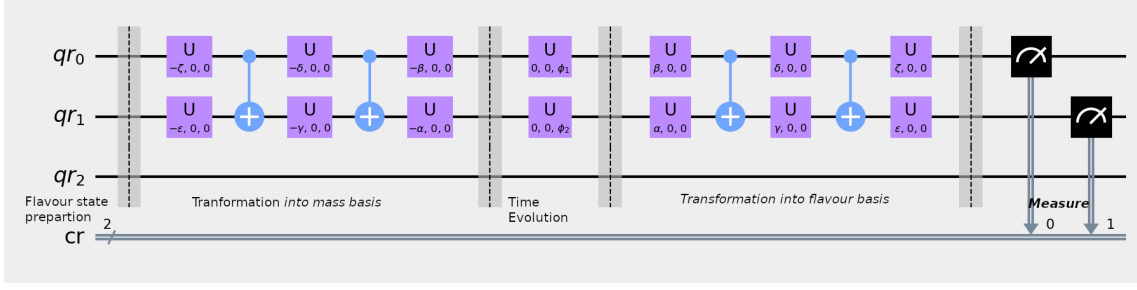


Figure 4.3: Circuit for simulating three flavour oscillation[1]

It should be noted that, this circuit is complex compared to two flavour case. Consequently read out errors and gate error will be more compared to the former. Also this circuit can be also extended to incorporate sterile neutrinos and to study matter effects (MSW effects). Scheme for such studies are also provided in [1].

4.3 Measuring Entanglement Using Simulation

For a two-flavour case, if the system we consider is electron-muon system, then linear entropy gives the entanglement in the system (refer section [3.5]).

$$S_{L\alpha}^{(e;\mu)} = S_{L\alpha}^{(\mu;e)} = 4|\tilde{\mathbf{U}}_{\alpha e}(t)|^2 |\tilde{\mathbf{U}}_{\alpha \mu}(t)|^2$$

From equation (3.4),

$$P_{\nu_\alpha \rightarrow \nu_\beta}(t) = |\langle \nu_\beta | \nu_\alpha(t) \rangle|^2 = |\tilde{\mathbf{U}}_{\alpha \beta}(t)|^2$$

Thus we can rewrite linear entropy as,

$$\begin{aligned} S_{Le}^{(e;\mu)} &= S_{Le}^{(\mu;e)} = 4P_{ee}P_{e\mu} \\ S_{L\mu}^{(e;\mu)} &= S_{L\mu}^{(\mu;e)} = 4P_{\mu e}P_{\mu\mu} \end{aligned} \quad (4.12)$$

Where $P_{\alpha\beta} = P_{\nu_\alpha \rightarrow \nu_\beta} = P_{\beta\alpha}$. We can get the appearance and disappearance probability in $e - \mu$ system directly from the circuit given in the figure 4.1. Substituting these values would give the linear entropy of the subsystems and thereby the entanglement of the system.

Similarly for three flavour case,

$$\begin{aligned} S_{Le}^{(e,\mu;\tau)} &= 4P_{e\tau}(P_{ee} + P_{e\mu}) = 4P_{e\tau}(1 - P_{e\tau}) \\ S_{L\mu}^{(e,\mu;\tau)} &= 4P_{\mu\tau}(P_{\mu e} + P_{\mu\mu}) = 4P_{\mu\tau}(1 - 4P_{\mu\tau}) \\ S_{L\tau}^{(e,\mu;\tau)} &= 4P_{\tau\tau}(P_{\tau e} + P_{\tau\mu}) = 4P_{\tau\tau}(1 - 4P_{\tau\tau}) \end{aligned} \quad (4.13)$$

Similarly we found out equations for other bi-partitions by permuting over the indexes e, μ, τ . From it, we can find out average linear entropy as,

$$\begin{aligned}\langle S_{Le}^{(2:1)} \rangle &= \frac{8}{3}(P_{ee}P_{e\mu} + P_{ee}P_{e\tau} + P_{e\mu}P_{e\tau}) \\ \langle S_{L\mu}^{(2:1)} \rangle &= \frac{8}{3}(P_{\mu e}P_{\mu\mu} + P_{\mu e}P_{\mu\tau} + P_{\mu\mu}P_{\mu\tau}) \\ \langle S_{L\tau}^{(2:1)} \rangle &= \frac{8}{3}(P_{\tau e}P_{\tau\mu} + P_{\tau e}P_{\tau\tau} + P_{\tau\mu}P_{\tau\tau})\end{aligned}\tag{4.14}$$

This can be calculated using the circuit given in the figure 4.3. Average linear entropy would give the global entanglement of the three-flavour system.

Chapter 5

Simulation Results

We used IBM Quantum Experience which is a cloud-based computing service provided by IBM to run our circuits. IBM Q (short form of IBM Quantum Experience) provides about 27 quantum services which comprise of 5 different types of simulators (including QASM Simulator) and 22 Quantum computers. Out of the 22 Quantum Computers, 9 are publicly accessible and the remaining are exclusive for the collaborators. Even though great advancement has been made in this field over the decade, still technology remains imperfect. Each gate applied to the circuit would induce an error of $\mathcal{O}(0.1\%)$. Readout error is of $\mathcal{O}(5\%)$ per qubit. Thus the error in the result increases as the length of the circuit, prohibiting lengthy calculations. But one can use quantum error-correcting codes to mitigate the errors.

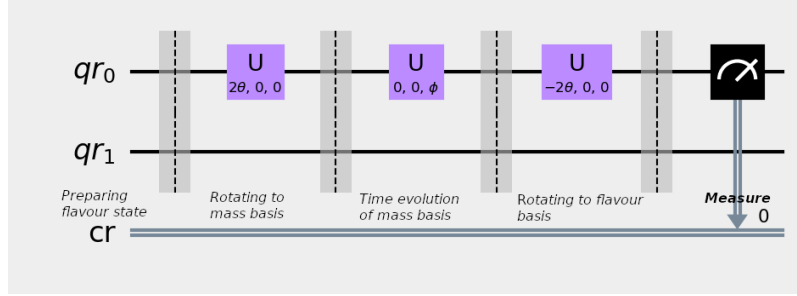
5.1 Two Flavour Oscillations: Simulation Results

With the quantum circuit defined in the section 4.1, we simulated an electron neutrino (ν_e) disappearance experiment with the parameters given by the KamLAND experiment [62]. Kamioka Liquid Scintillator Antineutrino Detector(KamLAND) is an electron antineutrino detector located in the Kamioka observatory. It studies neutrino oscillation using electron antineutrino produced by nuclear reactors.[63].

5.1.1 Simulation Using QASM Simulator

Electron neutrino state is encoded into $|0\rangle$ state. We run 1024 trials and got back the neutrino state after time evolution. Then we perform projective measurement. By projective measurement we means that output state is projected in to the compu-

tational basis ($\{|0\rangle, |1\rangle\}$). Thus the state is projected either to $|0\rangle$ or $|1\rangle$ depending upon output state. Here we run 1024 trials and takes the count of $|0\rangle$ state. From this count, disappearance probability of electron was calculated. The experiment was repeated for a range of neutrino beam energies and curve showing how disappearance probability varies with energy was plotted.



We performed simulations for different values of neutrino beam energy while fixing the L to be constant. We plotted how disappearance probability varies as a function of Energy in MeV. It should be noted that we had chosen $L = 180$ km in order to match the experimental conditions of the KamLAND.

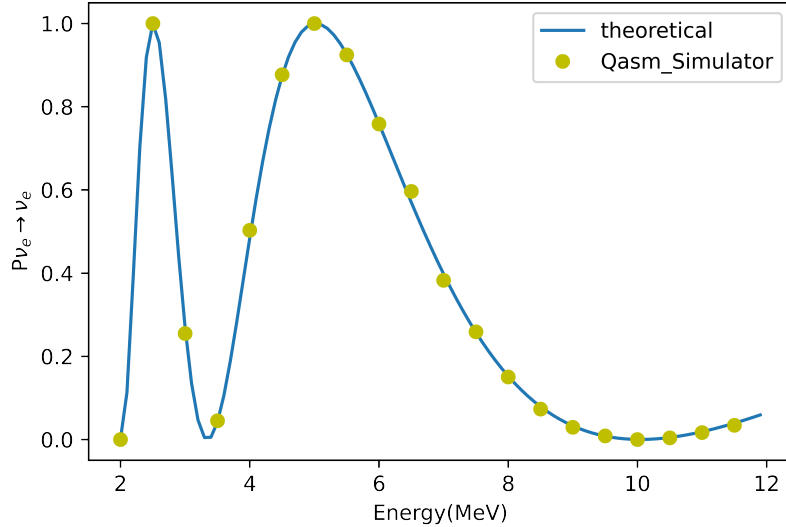


Figure 5.1: Disappearance probability in $e - \mu$ system as a function of energy (in QASM simulator).

From the figure 5.1 it is evident that our circuit performs very well and correctly predicts the disappearance probability. We were able to observe the sinusoidal variation of probability as predicted by equation (4.1). In the QASM simulator circuit perform extremely well and predicts probability that agrees with the theoretical value.

5.1.2 Simulation Using IBM Quantum Computer

Circuit provided in figure 4.1 is used to perform simulation in IBM Quantum computers. We performed the simulation on a IBM quantum computer named as IBM Armonk. It is a single qubit quantum computer which also supports pulse mode.

IBM Armonk

Quantum Volume : 1

Processor: Canary r1.2

Basis gates: ID, RZ, SX, X

Avg. CNOT Error: N/A

Avg. Readout Error: 3.160e-2

Avg. T1: 172.93 μ s

Avg. T2: 344.85 μ s

Like the former, we run the circuit 1024 shots and found out neutrino counts. Using this counts calculated the disappearance probability.

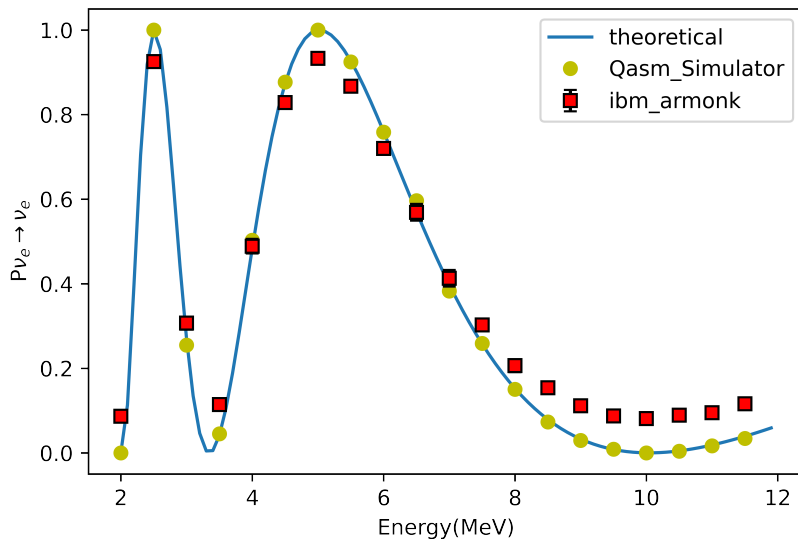


Figure 5.2: Disappearance probability in $e - \mu$ system as a function of energy (in Quantum computer)

Here we also have account for the statistical error that may happen while running circuits on actual quantum computers. For a particular value of energy we repeated the experiment for 10 times and calculated standard deviations of data. From figure 5.2 it is evident that the behaviour of theoretical curve by simulational results even though there is error in value predicted by the circuit.

5.1.3 Entanglement Studies

Through simulation using the circuit in figure 4.1, we can get the disappearance and appearance probability in the $e - \mu$ system. By substituting it back in the equation (4.12) we can find out the linear entropy of the system.

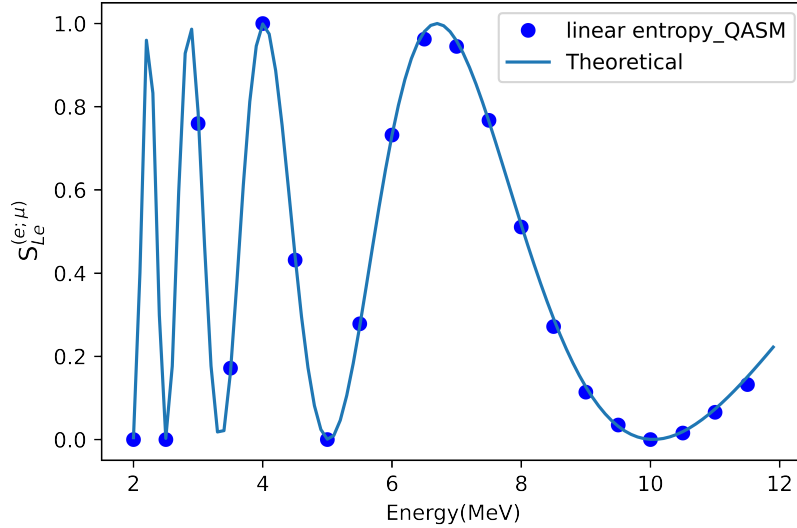


Figure 5.3: Linear entropy of $e - \mu$ system as a function of energy (in QASM simulator)

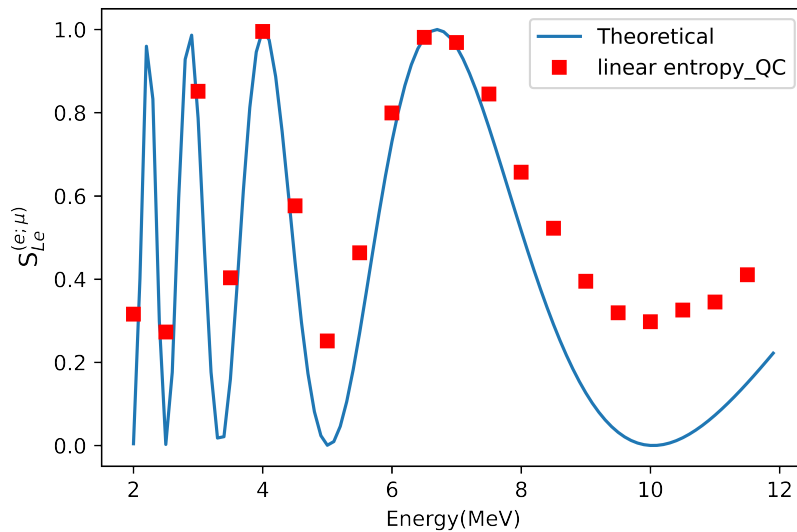


Figure 5.4: Linear entropy of $e - \mu$ system as a function of energy (in quantum computer)

From figure 5.3, it is clear that circuit predicts the linear entropy accurately in the QASM simulator. Here also, the error happening while performing simulation on actual quantum computer is visible (figure 5.4). Linear entropy as discussed earlier is a monotone of entanglement. Thus can be used as direct measure of entanglement in the system.

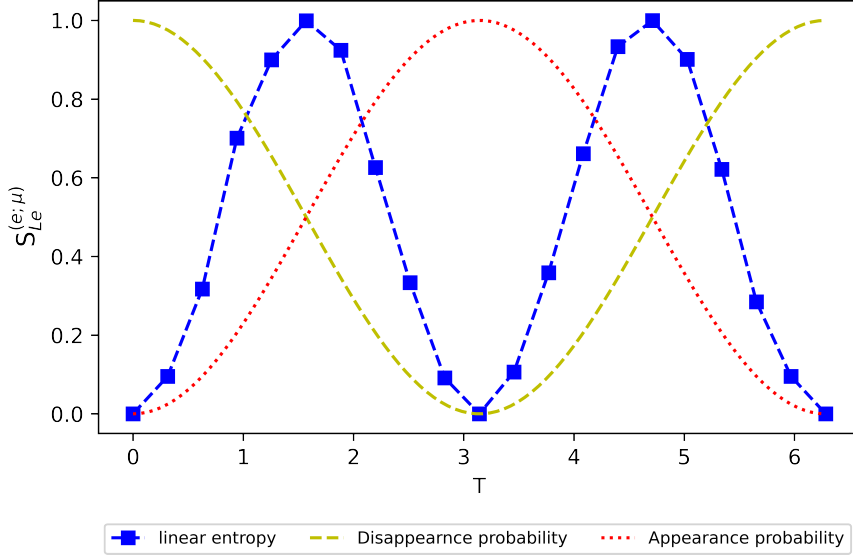


Figure 5.5: Entanglement in the $e - \mu$ system (in QASM simulator).

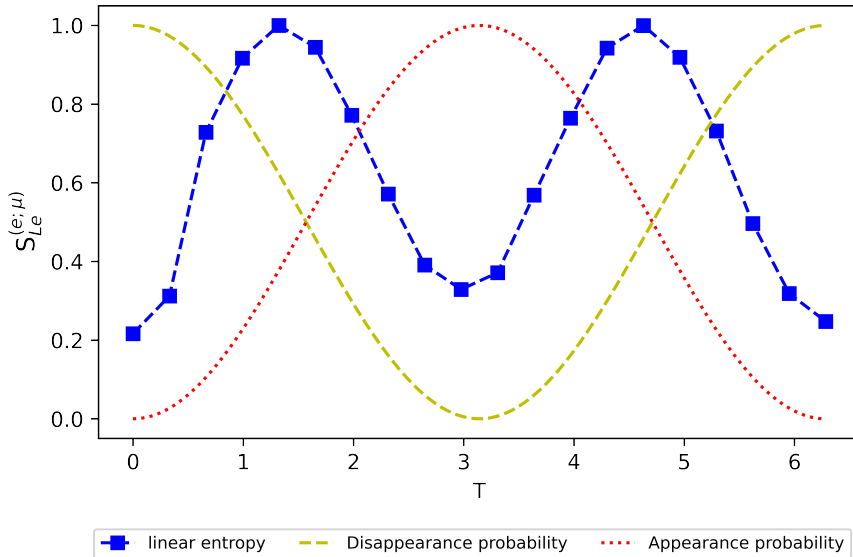


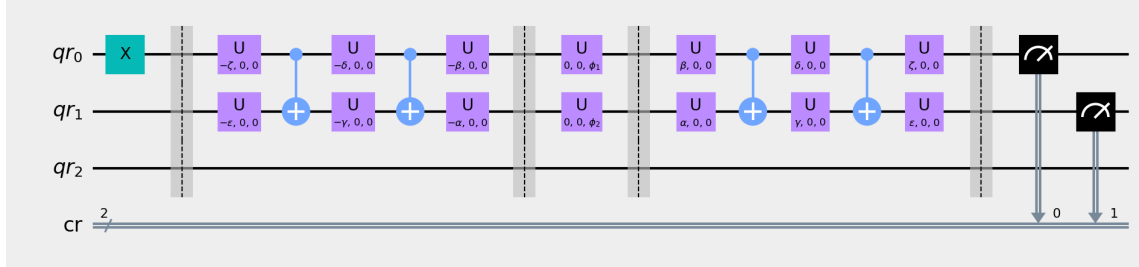
Figure 5.6: Entanglement in the $e - \mu$ system (in Quantum computer).

Here $T = \frac{\Delta m^2 t}{2E\hbar}$. If we fix the value of E , then T solely depend upon time t .

At $T = 0$, the disappearance probability ($P_{\nu_\mu \rightarrow \nu_\mu}$) is maximum and appearance probability ($P_{\nu_\mu \rightarrow \nu_\mu}$) is minimum. Thus system will have least entropy. As a result system will be least entangled. In our case, system behaves like a product state at $T = 0$. As time evolves (T increases), neutrinos began to undergo flavour oscillation. Appearance and disappearance probability show sinusoidal nature with time. Thus the linear entropy of the system varies in sinusoidal manner. Linear entropy is maximum when $P_{\nu_\mu \rightarrow \nu_\mu} = P_{\nu_\mu \rightarrow \nu_\mu} = 0.5$. Therefore, system will be maximally entangled at this value of T and minimum at $T = \pi$. This behaviour is clearly demonstrated in figures 5.5 and 5.6. Even though quantum computer gives the behaviour of system doesnot accurately the measure of entanglement.

5.2 Three Flavour Oscillation: Simulation Results

To perform three flavour oscillation we used the circuit given in the figure 4.3. We studied a system where all the neutrinos were of muon flavour initially. Through simulation we conducted appearance and disappearance experiments.



Here we prepare muon neutrino using the encoding scheme discussed earlier (equation 4.7),and then time evolved it. The output state is projected in to the basis $\{|00\rangle, |01\rangle, |10\rangle, |11\rangle\}$. We run the circuit 1024 times. Count of $|10\rangle$ state gives disappearance count of muon neutrino. Count of $|01\rangle$ and $|00\rangle$ gives the appearance count of tau and electron neutrino respectively. From these counts we can calculate corresponding probabilities.

Parameters required for simulation (mixing angle and mass square splittings) are taken from [61]. Simulations were performed on both the QASM simulator and the IBM Quantum computer.

5.2.1 Simulation Using QASM Simulator

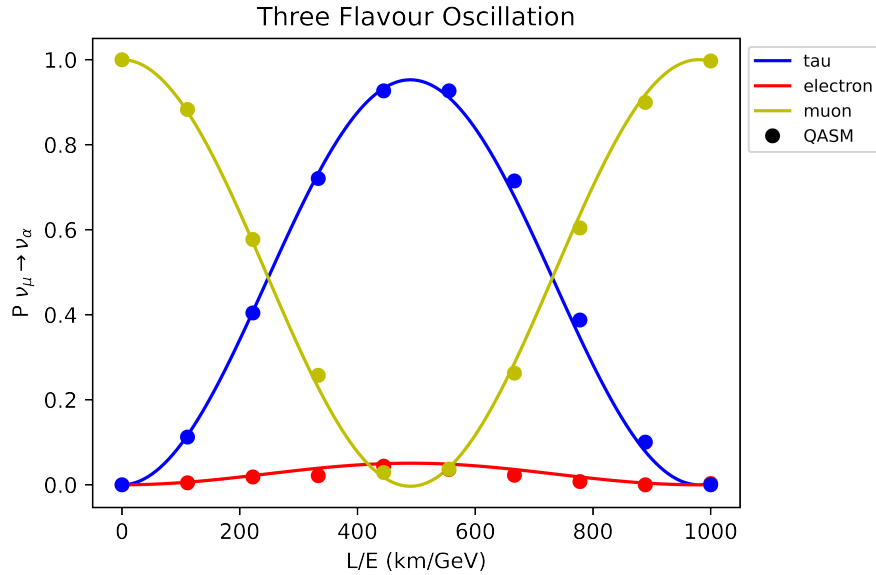


Figure 5.7: Three flavour oscillation probability as function of time (in QASM simulator)

Here in the Y axis we plot probability of transition from a muon flavour to a particular flavour α . It should be noted that alpha could be any flavour ($\alpha = e, \mu, \tau$). We calculated disappearance probability muon and appearance probability of electron and tau for various values $\frac{L}{E}$ with each experiment composed of 1024 trials. The plot showing how probabilities vary with $\frac{L}{E}$ is plotted. From the figure 5.7 it is clear that circuit works fine even though there are slight deviations can from theoretical value.

5.2.2 Simulation Using IBM Quantum Computer

The circuit was run on IBM Quantum computer named IBM Lima. It is a five qubit system.

IBM Lima

Quantum Volume : 8

Processor: Falcon r4

Basis gates: CX, ID, RZ, SX, X

Avg. CNOT Error: 1.220e-2

Avg. Readout Error: 3.860e-2

Avg. T1: 76.74 μ s

Avg. T2: 73.74 μ s

We performed 1024 trials. We got back appearance and disappearance counts. Oscillation probabilities were founded from these counts and experiment was repeated for different $\frac{L}{E}$ values.

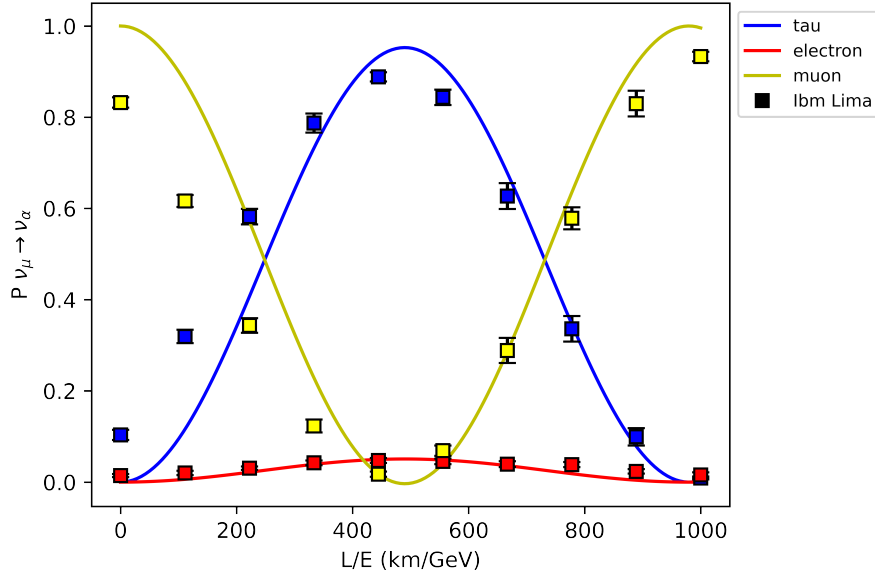


Figure 5.8: Three flavour oscillation probability as function of time (in Quantum computer)

Here we also have accounted for the statistical error that may happen while running circuits on actual quantum computers. For a particular value of $\frac{L}{E}$, we repeated the experiment 10 times and calculated standard deviations of data.

One can see deviations of oscillation probabilities predicted by the circuit from the actual value. As discussed above, the errors are due large length of the circuit. Compared to two flavour case, number of single qubit gates used is 5 times large and each gate approximately induce an error of $\mathcal{O}(0.1\%)$. This circuit also uses 4 two qubit gates which also induce errors into results. Further readout errors ($\mathcal{O}(5\%)$) can also influence final results. Also, due to T_1 and T_2 errore $|11\rangle$ have non zero counts in quantum computers. This affect the appearance and disappearance probabilities.

5.2.3 Entanglement Studies

Through simulation using the circuit in figure 4.3, we can get the disappearance and appearance probability in a three flavour system. We can use this data to find out the linear entropy.

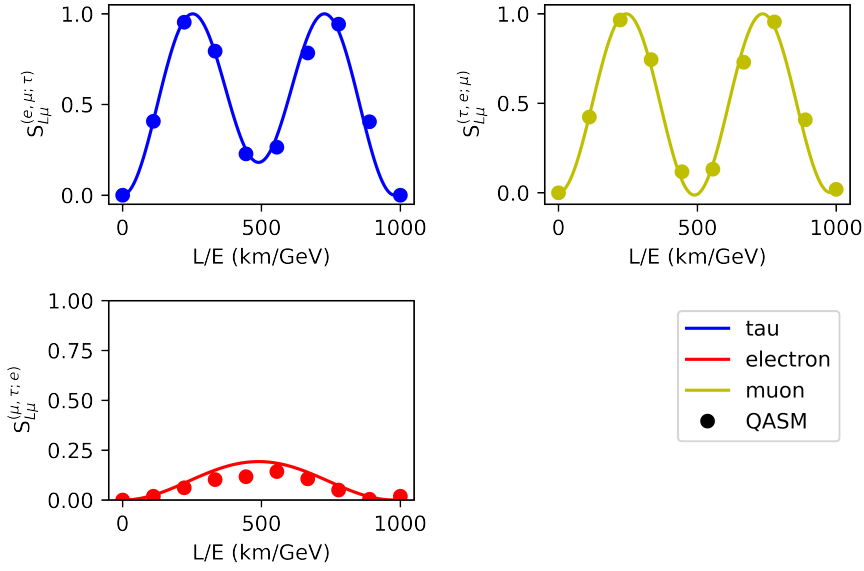


Figure 5.9: Linear entropy of 3-flavour system as a function of energy (in QASM simulator)

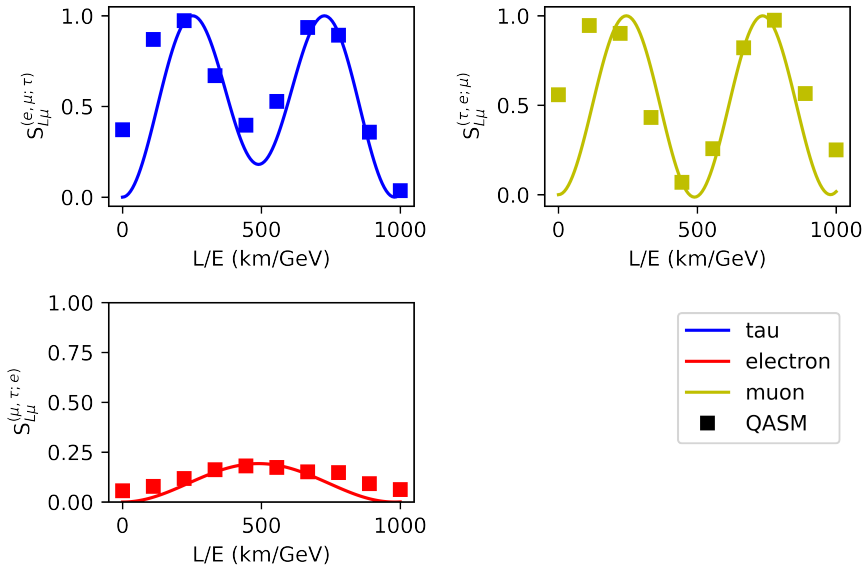


Figure 5.10: Linear entropy of 3-flavour system as a function of energy (in quantum computer)

In the figure 5.9, the first subplot represent $e\mu - \tau$ system. We partition the system into two subsystem. One composed of electron-muon flavour and other composed of tau flavour. This is done by tracing out tau flavour from the density matrix. Thus using the reduced density matrix of tau, we find out linear entropy the

total system ($S_{L\mu}^{(e,\mu;\tau)}$). Similarly, second and third subplots gives linear entropy of the systems after tracing out muon ($S_{L\mu}^{(\tau,e;\mu)}$) and electron neutrino ($S_{L\mu}^{(\mu,\tau;e)}$) respectively. The circuit predicts the linear entropy almost accurately in the QASM simulator. But while performing simulation on actual quantum computer error arises (figure 5.10). Using the linear entropy, we can calculate the average linear entropy of total system. This act as a measure of Global entanglement in the system.

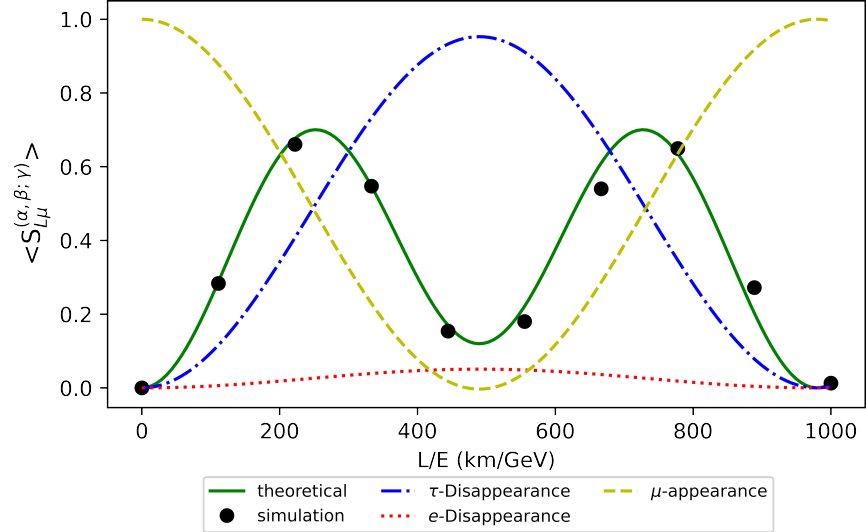


Figure 5.11: Global entanglement in the 3-flavour system (in QASM simulator).

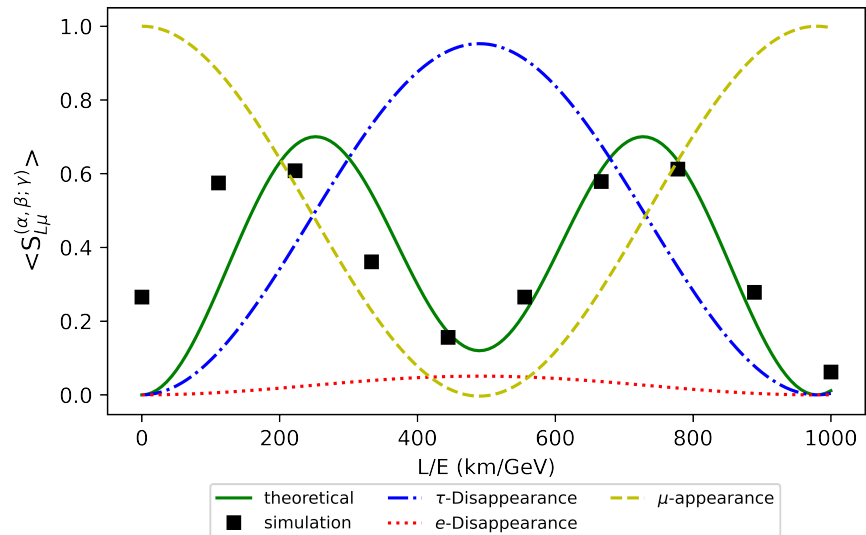


Figure 5.12: Global entanglement in the 3-flavour system (in Quantum computer).

Here $\langle S_{L\mu}^{(\alpha,\beta,\gamma)} \rangle$ = Average linear entropy of the system. Average linear entropy

is found out by considering all possible bi-partitions of the system. It is plotted as function of $\frac{L}{E}$. At constant value of E , average entropy solely depends upon L . In natural units $L = t$. Thus, at $t = 0$ disappearance probability of muon is maximum. As a result, the average linear entropy of the system of the system will zero. So that the flavour state at $t = 0$ is not entangled (product state). Now as time progresses flavour oscillation happens and as a result average linear entropy will vary. The global entanglement will be maximum when all oscillation probabilities (appearance and disappearance) together maximized.

Bibliography

- [1] C. A. Argüelles and B. J. P. Jones. Neutrino oscillations in a quantum processor. *Phys. Rev. Research*, 1:033176, Dec 2019.
- [2] Richard P. Feynman. Simulating physics with computers. *International Journal of Theoretical Physics*, 21(6-7):467–488, June 1982.
- [3] Michael A. Nielsen and Isaac L. Chuang. *Quantum Computation and Quantum Information: 10th Anniversary Edition*. Cambridge University Press, 2010.
- [4] Masuo Suzuki. Quantum monte carlo methods and general decomposition theory of exponential operators and symplectic integrators. *Physica A: Statistical Mechanics and its Applications*, 205(1):65–79, 1994.
- [5] Matthias Troyer and Uwe-Jens Wiese. Computational complexity and fundamental limitations to fermionic quantum monte carlo simulations. *Phys. Rev. Lett.*, 94:170201, May 2005.
- [6] I. M. Georgescu, S. Ashhab, and Franco Nori. Quantum simulation. *Rev. Mod. Phys.*, 86:153–185, Mar 2014.
- [7] Nathan Argaman and Guy Makov. Density functional theory: An introduction. *American Journal of Physics*, 68(1):69–79, 2000.
- [8] R J Bartlett. Many-body perturbation theory and coupled cluster theory for electron correlation in molecules. *Annual Review of Physical Chemistry*, 32(1):359–401, 1981.
- [9] S. Lloyd. Universal Quantum Simulators. *Science*, 273(5278):1073–1078, August 1996.
- [10] Raymond Davis, Don S. Harmer, and Kenneth C. Hoffman. Search for neutrinos from the sun. *Phys. Rev. Lett.*, 20:1205–1209, May 1968.
- [11] B. Pontecorvo. Mesonium and anti-mesonium. *Sov. Phys. JETP*, 6:429, 1957.

- [12] Ziro Maki, Masami Nakagawa, and Shoichi Sakata. Remarks on the unified model of elementary particles. *Prog. Theor. Phys.*, 28:870–880, 1962.
- [13] B. Pontecorvo. Neutrino Experiments and the Problem of Conservation of Leptonic Charge. *Zh. Eksp. Teor. Fiz.*, 53:1717–1725, 1967.
- [14] Arthur B. McDonald, Joshua R. Klein, and David L. Wark. Solving the Solar Neutrino Problem. *Scientific American*, 288(4):40–49, April 2003.
- [15] Daniel S. Abrams and Seth Lloyd. Quantum Algorithm Providing Exponential Speed Increase for Finding Eigenvalues and Eigenvectors. *Physical Review Letters*, 83(24):5162–5165, December 1999.
- [16] A. Aspuru-Guzik. Simulated Quantum Computation of Molecular Energies. *Science*, 309(5741):1704–1707, September 2005.
- [17] Daniel A. Lidar and Ofer Biham. Simulating ising spin glasses on a quantum computer. *Phys. Rev. E*, 56:3661–3681, Sep 1997.
- [18] David A. Meyer. Quantum computing classical physics. *Philosophical Transactions of the Royal Society of London. Series A: Mathematical, Physical and Engineering Sciences*, 360(1792):395–405, March 2002.
- [19] Siddhartha Sinha and Peter Russer. Quantum computing algorithm for electromagnetic field simulation. *Quantum Information Processing*, 9(3):385–404, June 2010.
- [20] M. Blasone, F. Dell'Anno, S. De Siena, M. Di Mauro, and F. Illuminati. Multipartite entangled states in particle mixing. *Phys. Rev. D*, 77:096002, May 2008.
- [21] M. Blasone, F. Dell'Anno, S. De Siena, and F. Illuminati. Entanglement in neutrino oscillations. *EPL (Europhysics Letters)*, 85(5):50002, mar 2009.
- [22] Massimo Blasone, Fabio Dell'Anno, Silvio De Siena, and Fabrizio Illuminati. On entanglement in neutrino mixing and oscillations. *J. Phys. Conf. Ser.*, 237:012007, 2010.
- [23] Massimo Blasone, Fabio Dell'Anno, Silvio De Siena, and Fabrizio Illuminati. A field-theoretical approach to entanglement in neutrino mixing and oscillations. *EPL (Europhysics Letters)*, 106(3):30002, may 2014.
- [24] S. J. van Enk. Entanglement of electromagnetic fields. *Phys. Rev. A*, 67:022303, Feb 2003.

- [25] S. J. van Enk. Single-particle entanglement. *Phys. Rev. A*, 72:064306, Dec 2005.
- [26] S. J. van Enk. Reply to “comment on ‘single-particle entanglement’ ”. *Phys. Rev. A*, 74:026302, Aug 2006.
- [27] Lee A. Rozema, Dylan H. Mahler, Alex Hayat, Peter S. Turner, and Aephraim M. Steinberg. Quantum data compression of a qubit ensemble. *Phys. Rev. Lett.*, 113:160504, Oct 2014.
- [28] Katherine L. Brown, William J. Munro, and Vivien M. Kendon. Using quantum computers for quantum simulation. *Entropy*, 12(11):2268–2307, 2010.
- [29] Craig R. Clark, Tzvetan S. Metodi, Samuel D. Gasster, and Kenneth R. Brown. Resource requirements for fault-tolerant quantum simulation: The ground state of the transverse ising model. *Phys. Rev. A*, 79:062314, Jun 2009.
- [30] T. F. Havel, S. S. Somaroo, C.-H. Tseng, and D. G. Cory. Principles and Demonstrations of Quantum Information Processing by NMR Spectroscopy. *Applicable Algebra in Engineering, Communication and Computing*, 10(4-5):339–374, May 2000.
- [31] F. Verstraete, D. Porras, and J. I. Cirac. Density matrix renormalization group and periodic boundary conditions: A quantum information perspective. *Phys. Rev. Lett.*, 93:227205, Nov 2004.
- [32] K. Temme, T. J. Osborne, K. G. Vollbrecht, D. Poulin, and F. Verstraete. Quantum Metropolis sampling. *Nature*, 471(7336):87–90, March 2011.
- [33] P.A. Zyla et al. Review of Particle Physics. *PTEP*, 2020(8):083C01, 2020.
- [34] F. P. An, A. B. Balantekin, H. R. Band, et al. Search for a light sterile neutrino at daya bay. *Phys. Rev. Lett.*, 113:141802, Oct 2014.
- [35] A. A. Aguilar-Arevalo, B. C. Brown, L. Bugel, G. Cheng, et al. Significant excess of electronlike events in the miniboone short-baseline neutrino experiment. *Phys. Rev. Lett.*, 121:221801, Nov 2018.
- [36] Carlo Giunti. Theory of Neutrino Oscillations. *arXiv:hep-ph/0311241*, February 2004. arXiv: hep-ph/0311241.
- [37] L. Stodolsky. When the wavepacket is unnecessary. *Phys. Rev. D*, 58:036006, Jul 1998.
- [38] Harry J. Lipkin. Stodolsky’s theorem and neutrino oscillation phases for pedestrians. 12 2002.

- [39] L. B. Okun, M. G. Schepkin, and I. S. Tsukerman. On the extra factor of two in the phase of neutrino oscillations. *Nucl. Phys. B*, 650:443–446, 2003. [Erratum: Nucl.Phys.B 656, 255–255 (2003)].
- [40] C. Giunti, C. W. Kim, and U. W. Lee. When do neutrinos really oscillate? quantum mechanics of neutrino oscillations. *Phys. Rev. D*, 44:3635–3640, Dec 1991.
- [41] C. Giunti and C. W. Kim. Coherence of neutrino oscillations in the wave packet approach. *Phys. Rev. D*, 58:017301, Jun 1998.
- [42] C. Giunti. Coherence and wave packets in neutrino oscillations. *Found. Phys. Lett.*, 17:103–124, 2004.
- [43] Giuliano Benenti, Giulio Casati, Davide Rossini, and Giuliano Strini. *Principles of Quantum Computation and Information: A Comprehensive Textbook*. WORLD SCIENTIFIC, December 2018.
- [44] A. Einstein, B. Podolsky, and N. Rosen. Can quantum-mechanical description of physical reality be considered complete? *Phys. Rev.*, 47:777–780, May 1935.
- [45] J. S. Bell. On the einstein podolsky rosen paradox. *Physics Physique Fizika*, 1:195–200, Nov 1964.
- [46] Alain Aspect, Philippe Grangier, and Gérard Roger. Experimental realization of einstein-podolsky-rosen-bohm gedankenexperiment: A new violation of bell’s inequalities. *Phys. Rev. Lett.*, 49:91–94, Jul 1982.
- [47] Alain Aspect, Jean Dalibard, and Gérard Roger. Experimental test of bell’s inequalities using time-varying analyzers. *Phys. Rev. Lett.*, 49:1804–1807, Dec 1982.
- [48] Charles H. Bennett, Herbert J. Bernstein, Sandu Popescu, and Benjamin Schumacher. Concentrating partial entanglement by local operations. *Phys. Rev. A*, 53:2046–2052, Apr 1996.
- [49] Charles H. Bennett, Gilles Brassard, Sandu Popescu, Benjamin Schumacher, John A. Smolin, and William K. Wootters. Purification of noisy entanglement and faithful teleportation via noisy channels. *Phys. Rev. Lett.*, 76:722–725, Jan 1996.
- [50] Sandu Popescu and Daniel Rohrlich. Thermodynamics and the measure of entanglement. *Phys. Rev. A*, 56:R3319–R3321, Nov 1997.

- [51] Jae-Weon Lee, Eok Kyun Lee, Yong Wook Chung, Hai-Woong Lee, and Jaewan Kim. Quantum cryptography using single-particle entanglement. *Physical Review A*, 68(1):012324, July 2003.
- [52] Egilberto Lombardi, Fabio Sciarrino, Sandu Popescu, and Francesco De Martini. Teleportation of a vacuum–one-photon qubit. *Phys. Rev. Lett.*, 88:070402, Jan 2002.
- [53] Björn Hessmo, Pavel Usachev, Hoshang Heydari, and Gunnar Björk. Experimental Demonstration of Single Photon Nonlocality. *Physical Review Letters*, 92(18):180401, May 2004.
- [54] William K. Wootters. Entanglement of formation and concurrence. *Quantum Information and Computation*, 1(1):27–44, July 2001.
- [55] Charles H. Bennett, David P. DiVincenzo, John A. Smolin, and William K. Wootters. Mixed state entanglement and quantum error correction. *Phys. Rev. A*, 54:3824–3851, 1996.
- [56] Ryszard Horodecki, Paweł Horodecki, Michał Horodecki, and Karol Horodecki. Quantum entanglement. *Rev. Mod. Phys.*, 81:865–942, Jun 2009.
- [57] Luigi Amico, Rosario Fazio, Andreas Osterloh, and Vlatko Vedral. Entanglement in many-body systems. *Rev. Mod. Phys.*, 80:517–576, May 2008.
- [58] Gavin K. Brennen. An observable measure of entanglement for pure states of multi-qubit systems. *arXiv:quant-ph/0305094*, November 2003. arXiv: quant-ph/0305094.
- [59] Carlo Giunti and Chung W. Kim. *Fundamentals of Neutrino Physics and Astrophysics*. 2007.
- [60] C. Giunti. No effect of majorana phases in neutrino oscillations. *Physics Letters B*, 686(1):41–43, 2010.
- [61] Ivan Esteban, M. C. Gonzalez-Garcia, Alvaro Hernandez-Cabezudo, Michele Maltoni, and Thomas Schwetz. Global analysis of three-flavour neutrino oscillations: synergies and tensions in the determination of θ_{23} , δ_{CP} , and the mass ordering. *JHEP*, 01:106, 2019.
- [62] K. Eguchi et al. First results from kamland: Evidence for reactor antineutrino disappearance. *Phys. Rev. Lett.*, 90:021802, Jan 2003.
- [63] Toshiyuki Iwamoto. Measurement of Reactor Anti-Neutrino Disappearance in KamLAND. Other thesis, 2 2003.